ANSWER TO COMMENTS FOR REFEREE #1.

The present authors' comment, referring to the discussion paper titled "Lituya Bay 1958 Tsunami – detailed pre-event bathymetry reconstruction and 3D-numerical modelling utilizing the CFD software Flow-3D", is aimed at the comment of anonymous referee #1, published on 11 November 2019.

Authors:
Dear referee,
we thank you very much for the time spent in reviewing our work and for the very good advices to further improve the manuscript. We have taken care of your comments and provided improvements as suggested. Results have been updated where changes in the modeling outputs or new findings raised during the major revision of the work.

Please refer to the **marked-up manuscript version** (page 19 of the current pdf.file)**,** where changes are highlighted for the new manuscript version compared to the old one:
- Corrections and improvements: Bold light green
- Deleted sentences and words: Underlined red

Following the references, we show figures and tables that have been added, updated or deleted.
See from page 30.

The authors comment on the referee advices as follows:

(1)
Referee:
Reference cited in l10 correspond to the year 2019, not to 2018.

Authors:
Thank you for this notice, we have provided the correction.
See page 2 line 9.

(2)
Referee:
My point here is the concept of what is called "denser fluid". As it's recalled in the paper, Pararas Carayannis classify this slide as a "subaerial rockfall" while Miller describes it as a slide in a midway between a landslide and a rockslide. The use of a "denser fluid" to recreate the slide is an approximation to the modelling of this event, nevertheless it should be remarked that the authors modelling is nearer to the Miller and Fritz approximation as a landslide.

Authors:
We have remarked this important information, where we will state in the model set up chapter that our sliding model concept is, as you highlight, nearer to the slide model described by Miller and Fritz.
See page 10, line 11.

In particular we have specified better the task of this work, where we have underlined that to recreate the sliding process considering the real physical behavior of the rockslide (so considering its rheology) is not a focus of this study.
See page 3, line 15.

Thus we have justified our decision to adopt this simple concept of the denser fluid to initiate the wave formation with a comparable impact intensity.
See page 3, line 25
See page 10, line 40.

(3)
Referee:
In this sense, as authors remark, the used model is limited as authors must add a virtual wall on one side to avoid the spreading of the sliding mass during the landslide. Is there a remarkable difference if this wall is not considered?

Authors:
In this work we focus on the wave dynamics, where the sliding fluid volume represents the trigger process to initiate the wave generation and propagation. So, since we are not interested in perfectly reproducing the physics of the rockslide with its rheology, we adopted the simplified concept of the "denser fluid" compared to the sea water to recreate a sliding mass on a slope with a comparable impact behavior, with the possibility to adapt its shape according to the topographic surfaces.
The use of the virtual walls and their effects has been analyzed in the preliminary simulations.
See page 13, line 18.

The absence of the walls allows the fluid mass to spread during the collapse process, while the presence of the walls constricts the fluid mass until the impact into the sea. This mostly influences the wave features during the propagation phase and the further run-up on the opposite slope respect the slide source.
See page 13, line 28.
See page 18, line 40.

In the case of the simulations with the topographic surface, on the SE border of the detachment area the topography acts like a natural constriction for the dense fluid.
See figure 7 at page 34.
See page 19, line 4.

While on the NW border the presence of the wall has been adopted as a simple solution to compensate the lack of topographic elements due to the presence of scars related to secondary rockslides not involved in the wave generation.
See page 19, line 5.

From our understanding almost all the main rockslide volume impacts the water body and generates the impulse wave. The presence of the virtual wall avoids the lack of part of the collapsing dense fluid volume to impact the water body, that would, on the contrary, spread and impact on the glacier, resulting in a decrease of the wave feature and thus on the run-up process.
This aspect has been clarified and discussed in the discussion chapter.
See page 18, line 40.

(4)
Referee:
As different roughness values are used I would like to see how this friction is parameterized in the model.

Authors:
Surface roughness in Flow-3D basically consists of two components. The first results from the processing of the considered solid structures (stl-files) with the FAVOR-method during the preprocessing procedure. Depending on mesh structure and size, the computation geometry is delivered and it features minor divergences from the original solid structure. For the case that the mesh orientation does not perfectly fit with surface slope the computation geometry typically features a minorly rougher surface than the solid structure.
Secondly, a roughness height can be additionally determined for every considered solid structure. It is defined as the equivalent grain roughness with the dimension of a length (m).
In this case the purpose was to represent the roughness due to vegetation.
This background information on the roughness in Flow-3D is reported in the manuscript in the model description chapter.
See page 12, line 18.

We have provided a more detailed discussion on the influence of surface roughness on the modelling results in the results and discussion chapter.
See page 18, line 13.
See page 20, line 29.

For it, further simulations have been accomplished as well and thus new results are reported in the manuscript.
See figure 12c at page 40.

(5)
Referee:
In this section and later, authors describe the computation time that takes the different simulations. Although it’s a useful relative value if we compare the different computation times described along the paper, I would like to know what computational resources are used in order to imagine the real computational effort needed to reproduce these experiments.

Authors:
Please find in here the requested information on computational resources that have been added to the manuscript:
- Processor: Inter® Core™ i7-3820 CPU 3.60 GHz
- RAM: 32.0 GB
- System type: 64-bit Operating System
- Graphic card: GeForce GTX 6602 (Integrated RAMDAC, total available memory 4096 MB)
- Number of core license tokens checked out: 8 (Flow-3D parallel license code)

See page 10, line 20

(6)
Referee:
Again, in p13, l9-10 authors speak about computational time. With the same computational resources as before?
Again, same question about computation times in p14, l17-18.

Authors:
For all simulation the same computational resource has been used (for details see issue (5))
As well this is clarified this in the manuscript
See page 10, line 20
See page 13, line 12.
See page 16, line 29.

(7)
Referee:
To my view, the discussion presented in p15, l15-24 makes no much sense as the modelling process is approximating a rockslide or a landslide-rockslide by a landslide by means of a "denser fluid". If you don't want to remove this paragraph I would suggest remarking that this simulation of the submerged propagation of materials would not valid for the Lituya Bay event unless it would be considered as a pure landslide event.

Authors:
In this section we presented the propagation of the sliding fluid on the bay floor as an application available in Flow-3D to observe the mixture process between two fluids with different density, an application that can be adopted also to observe natural phenomena.
We fully agree that it is not correct to state that we are observing the propagation of the rockslide material along the bay floor. We are analyzing the mixture process of two fluids with different densities.
We have clarified this aspect in the manuscript and considered being consistent with terminology.
See page 18, line 21.
See page 21, line 21.

Additionally, we have decided to skip the (old) figure 13 (denser fluid spreading under water) since it is not relevant for this study (and not physically correct).
See page 50, line 10.

We have used the term "rockslide" when referring to literature and to the observed processes. The terms "denser fluid" and "fluid mixing process" are used when referring to the current modelling approach.
See page 1, line 13,18,19,25.
See page 2, line 9,12,21.
See page 3, line 17,23,24,26,27,29.
See page 4, line 29,32,35,36.
See page 5, line 2,11,33,34.
See page 7, line 6,18,19,20.
See page 8, line 14.
See page 10, line 8,9,26,30,35,36,38,39.
See page 11, line10,11,39.
See page 12, line 32,34,38.
See page 13, line 6,9 24.
See page 14, line 5,7,10,28,32,40.
See page 15, line 14,18,24,29,35,39.
See page 16, line 1,39.
See page 17, line 24.

See page 18, line 21,23,25.
See page 19, line 7,8,9,19,21.
See page 21, line 10,14,21,22,24.
See page 22, line 14,27,33.
See page 23, line8.
See page 24, line 5.
See figure 14 at page 41.

(8)
Referee:
In p17, l3-8, authors discuss that they don't find differences nor in inundation neither in the trimline with different roughness values from 0-3m. I can understand these results around steeper areas, but are there no differences in the Fish Lake area? What about around the Eastern flat area around the Paps? I cannot understand how the model doesn't provide larger inundation areas around flat areas when the roughness values go to zero.

Authors:
We thank you very much for this important note. Discussion of your comment and re-analysis of our models set-up and results finally led to the fact that we could identify a (user) mistake in the parameterization of the roughness in Flow-3D. We double checked the model set up in order to verify that everything is correct.
New simulations have been ran in order to verify changes in outputs, thus to provide correct results for different values for roughness, in terms of inundation process. Concerning this aspect reference is made also to the authors comment on the review of referee#2 (issue (18)).
In the results chapter we have demonstrated the effect in use of different values of relative roughness for the topographic surface, where we have discussed the new results and show them in the figures.
See page 18, line 13.
See page 20, line 29.
See figure 12c at page 40.

(9)
Referee:
p18, l30-34. Please, remark that these conclusions should be valid for landslide simulations. In the case of rockslides, Flow-3D can offer good approximations but with the limitations of the physics included in the numerical model.
…
Just to change chapter by section in l37.

Authors:
We totally agree to these considerations and we have adopted changes in the conclusions where we more specifically focus on a correct use of terminology (see issue (7)) and a discussion of the limitations of the chosen modelling concept with regard to the representation of the physics of the landslide process.
In the new version of the manuscript we have stated in the introduction the main task of the work, where we specify our intention concerning the use of the specific model for the denser fluid.
See page 3, line 15.

Secondly we have remarked this aspect in the conclusion.
See page 23, line 34.

ANSWER TO COMMENTS FOR REFEREE #2.

The present authors' comment, referring to the discussion paper titled "Lituya Bay 1958 Tsunami – detailed pre-event bathymetry reconstruction and 3D-numerical modelling utilizing the CFD software Flow-3D", is aimed at the comment of anonymous referee #2, published on 20 November 2019.

Authors:
Dear referee,
we thank you very much for the time spent in reviewing our work and for the very good advices to further improve the manuscript. We have taken care of your comments and provided improvements as suggested. Results have been updated where changes in the modeling outputs or new findings raised during the major revision of the work.

Please refer to the **marked-up manuscript version** (page 19 of the current pdf.file)**,** where changes are highlighted for the new manuscript version compared to the old one:
- Corrections and improvements: Bold light green
- Deleted sentences and words: Underlined red

Following the references, we show figures and tables that have been added, updated or deleted.
See from page 30.

The authors comment on the referee advices as follows:

(1)
Referee:
The manuscript would benefit from being shortened, citing existing literature rather than repeating. This is especially relevant for the first two sections (first 6 pages), that do not bring much new knowledge.

Authors:
In the first pages of the manuscript the idea was to summarize the work that has been done by now on the Lituya Bay tsunami event to give a general overview (without going too much into details) and to give the possibility to the reader to refer directly to the specific previous works on this topic. During manuscript revision, we cited better this first part of the manuscript in order to provide a shorter introduction to the reader without loss of the most relevant information. We decided to merge the subsection (2.3.1, 2.3.2 and 2.3.3) in one whole section 2.3 where relevant existing studies on the Lituya Bay tsunami case are briefly summarized.
See page 5, line 16.

(2)
Referee:
Some physical explanations are hard to follow (examples presented below).
…
Why do you say that a denser fluid is a suitable concept for the 1958 Lituya Bay rockslide? This must be substantiated from a discussion of rockslide rheology, which is presently completely left out. The slide is modelled as a Newtonian fluid (Navier-Stokes equations) and I would not call that a suitable concept for a rockslide. What is the "viscosity" of the rockslide?

Authors:
In this work the focus is set mainly on the wave dynamics (generation, propagation and inundation processes). Concerning the use of the “denser fluid”, approximating the rockslide at the bay head, the intention is to apply a simplified modelling concept which initiates the wave process in the way it was observed during the event. The simplified concept has to be applied here since there are modelling limitations of multi-hazards (hydraulic processes and gravitational hazards) within one software application.
We specified better the task of this work, where we underline that to recreate the sliding process considering the real physical behavior of the rockslide (so considering its rheology) is not a focus of this study. Thus we justify our decision to adopt this simple concept of the denser fluid to initiate the wave formation with a comparable impact intensity.
See page 3, line 15,25.
See page 10, line 40.

To be consistent with the terminology and the adopted (simplified) model we referred to the “denser fluid” (as a general concept) and not to the “rockslide”.
The terms “denser fluid” are used when referring to the current modelling approach.
We used the term “rockslide” when referring to literature and to the observed processes.
See page 1, line 13,18,19,25.
See page 2, line 9,12,21.
See page 3, line 17,23,24,26,27,29.
See page 4, line 29,32,35,36.
See page 5, line 2,11,33,34.
See page 7, line 6,18,19,20.
See page 8, line 14.
See page 10, line 8,9,26,30,35,36,38,39.
See page 11, line10,11,39.
See page 12, line 32,34,38.
See page 13, line 6,9 24.
See page 14, line 7,10,28,32,40.
See page 15, line 14,18,24,29,35,39.
See page 16, line 1,39.
See page 17, line 24.
See page 18, line 21,23,25.
See page 19, line 7,8,9,19,21.
See page 21, line 14,21,22,24.
See page 22, line 14,27,33.
See page 24, line 5.

In the case of the Lituya Bay, we can confirm that our concept worked well in initiating and reproducing the wave dynamics. We clarified this aspect of our work to make sure that the purpose is clearly understandable and to avoid other expectation from the reader.
See page 10, line 9,11.
See page 22, line 28.
See page 23, line 35.

Concerning the terminology in the manuscript, reference is made also to the authors comment on the review of referee#1 (issue (7)).

(3)
Referee:
Sensitivity to (spatial) grid resolution is mentioned in several places. It is not a new thing that results depend on the resolution. And it is not sufficient to conclude that a resolution of 15x15x10 m best reproduces the trimline. What if the resolution is even finer? Will the results

be further improved (or will spatial refinement even cause instability)? I am missing a regular convergence test quantifying the convergence rate, or (in 3D) at least a conformation that the differences are reduced between each refinement.

Authors:
We showed the results of simulations with different grid resolutions to highlight the difference in results and to investigate how hydraulics is affected by the adopted mesh size.
In the new manuscript we stated that the resolution of 15x15x10 m (adopting a relative roughness for the topographic surface of 2 m) is the one that well (not perfectly) reproduces the observed trimline within the computational limitations on a standard work station.
See page 10, line 20
See page 18, line 17.

Additionally, we state that also adopting a uniform grid resolution of 20 m the resulting trimline is well reproduced.
See page 18, line 19

With regard to the general complexity of the modelled processes and the involved uncertainties this quality of reproducing the observed processes is sufficient in our opinion, also in comparison to available numerical models in previous works.
See figure 12 at page 40.

At the time (and still, even the use of a more powerful machine) it has not been possible to simulate a model with a finer mesh due to the computational limitations, so it has not been possible to provide a more substantial analysis of convergence (or a conformation in difference reduction) related to the size of the mesh cells.
See page 20, line 3.

To verify improvements in results in function of the grid resolution, we have provided a conformation of difference reduction in flow characteristics values, between each refinement.
See page 19, line 32.

For this purpose, we have not focused on the run-up values or in the resulting trimline where 3D topographic effects can be very influential, but on the wave characteristics.
See page 20, line 4,8.
See figure 10 at page 37-38.
See figure 13 at page 41.

Any new findings have been considered in the revised manuscript, hopefully giving them more value and reliability.
See figure 12 at page 40.

(4)
Referee:
Some phrases are repeated several times (as e.g. the 524 m), possibly indicating that the structure of the paper is not optimal.
…
The linguistics of the manuscript should be improved (not further detailed below).

Authors:
Thank you for this notice. During revision, we have carefully checked the manuscript for repeated information and adapt accordingly.
See page 5, line 3, 33.
See page 6, line 34.
See page 9, line 10.

See page 14, line 20.
See page 20, line 35,38.

Moreover, we have improved language accuracy (see list at comment #2)
Concerning the structure of the manuscript and suggestions for improvement reference is made to issue (8).

(5)
Referee:
Be careful with terms like 'wave height' (crest-to-trough) and 'amplitude' (above equilibrium level for a harmonic wave). Better use e.g. 'surface elevation'.
…
Be careful with the use and definitions of terms like rock fall, rock avalanche, rockslide etc.

Authors:
Thank you for this advice, we have checked and provided changes in the terminology. We have used water surface elevation for general descriptions, wave amplitude when we referred to maximum values of flow height above the sea level, and wave height when this term is used in literature review.
See page 1, line 19.
See page 5, line 13.
See page 6, line 7,16,22,33.
See page 7, line 1,3,17.
See page 12, line 12,13.
See page 13, line24.
See page 15, line 25.
See page 16, line 8,9,30,40.
See page 17, line 3,6,11,16,33.
See page 18, line 4.
See page 19, line 10,23,36,38,41.
See page 22, line 31.
See page 23, line 10,11.
See figure 8 at page 35, line 3.
See figure 10 at page 38, line 5.

Concerning the terminology in the manuscript reference is made also to the authors comment on the review of referee#1 (issue (7)).

(6)
Referee:
p2, l20: Studies of rockslide tsunamis started long before Fritz et al. (2001), but the references listed here are perhaps meant to be relevant for the 1958 Lituya Bay event only?

Authors:
Yes, here only works related to the Lituya Bay case study are discussed. During manuscript revision, we have carefully checked the literature again.
See page 5, line 16.

(7)
Referee:
p2, l30: I do not agree that the questions listed here are all "open questions". Much work has already been done to answer them.

Authors:
We fully agree with this consideration. We have rephrased this sentence specifying that we want to give a further contribution to these research questions which have been raised and discussed within previous studies and which are relevant both for basic research and practice in multi hazards risk assessment.
See page 2, line 25.

(8)
Referee:
Would it be better to switch sections 2.1 and 2.2?

Authors:
Yes, for the reader it is probably clearer to get information on the case study characteristics first and a summary of the hazard event subsequently. We have switched the two chapters in the new manuscript.
See page 3, line 40.

(9)
Referee:
p4, l38: Better use 'head of the bay' rather than 'end of the bay'? At least be consistent throughout the text.

Authors:
In order to be consistent in terminology in the whole manuscript (compare issue (5)), we have used “head of the bay” in this context as suggested.
See page 4, line 5.
See page 14, line 30.
See page 17, line 39.
See page 23, line 4.

(10)
Referee:
p5, l12: What is the difference between physical scale tests and empirical studies? It seems like the terms are mixed further down (e.g. in p5, l34 and p6, l1 are mentioned experiments under the heading 'Empirical studies')

Authors:
Since we have summarized and shortened the first part of the manuscript, we adapted the section on the referred past works and thereby considered this issue. It is not always clear how to classify previous works in this context since empirical equations are often a result of experiments and related analyses.
During revision and shorting of the discussion of previous works we have merged the sections 2.3.1, 2.3.2. and 2.3.3.
See page 5, line 16.

(11)
Referee:
Section 2.3.3: Several previous studies are mentioned. However, for most of them it is not mentioned what equations are used, rendering the descriptions less useful. The importance of nonlinearity and dispersion should be elaborated.

Authors:
As we mention before, we wanted to give a general overview of the previous work on Lituya bay without entering too much in the details. To be consistent with the request to summarize the first 6 pages (see issue (1)) we suggest not to provide further details on previous studies or additional theory background.
See page 5, line 16.

(12)
Referee:
Section 3.1 might represent a valuable contribution, but is hard to follow.

Authors:
In recreating the topography and the pre-event bathymetry we wanted to summarize the descriptions and available information provided in previous works and, based on that, describe the processing of the pre-event terrain in our study.
We have tried to rephrase this section to make it clearer.
See section 3.1 at page 7, line 27.

(13)
Referee:
p7, l33: Volume is 3x108 m^3. p4, l13 and p7, l40 say 30x106 m^3. Please comment on this.

Authors:
As described in Ward and Day (2010), 3×10^8 m^3 is the total infill of the bay after the tsunami event, that included the rockslide material plus additional material coming from other sources (soil, subsoil from the inland, deltas, under glacier sediments etc.)
See page 8, line 9.

The volume of 30×10^6 m^3 is the one that has been estimated for the rockslide only (Miller 1960).
See page 4, line 36.

We have considered to make some improvements to avoid misunderstandings.

(14)
Referee:
Section 3.2.1: I would prefer to see what equations are solved. Also, first and the second order approach for the rockslide must be elaborated further already here (is this the order of the scheme for the phase/density transport equation?). The explanations that follows on p12 do not suffice either. p9: Much of the discussion is on turbulence and density, while slide-rheology is not mentioned at all. See also General Comments above.

Authors:
We have added the basic equations adopted in Flow-3D (e.g. RANS and VOF method) and additional explanation for a better understanding of the computational process, and to avoid confusion with other explanations.
See page 9, line 26.

We wanted to provide a basic and brief background on the density evaluation model without going to much in the details. We have rephrased this explanation to make it more clear for the reader.
See page 10, line 12,16 .

As mentioned previously, since it is not in our interest to recreate the rockslide physics, the rockslide rheology is thus not discussed (refer to answers to comment #2).

(15)
Referee:
p9, l16: "These models (first or second order) compute a separate transport equation for the density and simulate the movement of two different fluids (of different densities) in the domain." This is basically VOF methodology that is already mentioned in l3.

Authors:
We have provided better explanations and added the equations of the VOF method (separation between fluid and air in the computational cells) to avoid misunderstand with what have been reported for the density evaluation model (separation between two fluid with a different density), which definition is taken form the user´s manual of Flow-3D.
See page 9, line 26.
See page 10, line 12,16 .

(16)
Referee:
p10, l2: Cell size (relative to wave length and relative to temporal grid increment) is more important than number of cells.

Authors:
To show that we set our preliminary models on the base of the work of Basu et al (2010), we provided the same kind of information they provide (the number of cells for each axis) rather than the cell size.
For the revised simulation we have changed the cell size to a uniform size of 10 m for a better performance of the model concept analysis. Thus in the new manuscript we have specified the adopted cell size.
See page , line 15,16.

(17)
Referee:
p10, l35: Why outflow boundary conditions here? Why not accept reflections (from steep/closed boundaries)?

Authors:
Reflections are not considered to happen at the boundary locations of the domain. The outflow boundary condition is set to allow the wave to exit the domain as it is supposed to be on the floodplain and as well at La Chaussee Spit.
See page 10, line 18.
See page 11, line 6.

Reflections at the steep slopes around the bay are already due to the topographic effect and thus at these locations the mesh block boundaries are not relevant.
See page 10, line 19.
See page 16, line 35.

(18)
Referee:
p11, l6: Why does the "computational surface" have a sort of a roughness? This should be explained. A numerical "staircase slope" in a vertical transect will not pose the same kind of reflections as a "staircase no-flux boundary" in a horizontal projection.

Authors:
The computational surface of the considered solid bodies, which are implemented in Flow-3D as stl-files, are generated by use of the FAVOR-method during preprocessing. Based on the characteristics of the applied orthogonal mesh this computational surface is differing from the smooth surface as it is composed for this work by NURBS surface in Rhinoceros 6. It features a slightly rougher surface (staircase structure) which is treated as one component of the total surface roughness in Flow-3D.
Secondly an additional parameter (equivalent roughness height) can be attributed to the surface components in Flow-3D.
This background information on the roughness in Flow-3D is reported in the manuscript in the model description chapter.
See page 12, line 18.

We have provided a more detailed discussion on the influence of surface roughness on the modelling results in the results and discussion chapter.
See page 18, line 13.
See page 20, line 29.

For further comments on the roughness in Flow-3D reference is made to issue (29) and the authors comment on the review of referee#1 (issue (4)).

(19)
Referee:
p11, l23: The slide is slower for a steeper angle? This is counter intuitive and deserves some discussion. A longer travel distance does not "allow the slide more time to get higher speed". Or: what if the slope is zero? Without friction, both slides should have the same velocity at the end of the slope (v~sqrt(2*g*H)). Including friction, gentle (and longer) slopes means more energy lost to friction (Energy = Force x distance). This is especially the case for real cases, where friction is of Coulomb type and thus higher for more gentle slopes.

Authors:
We thank you very much for this important note. It is obvious that, according to basics in mechanics, end velocity of an obstacle sliding on an inclined plane is only related to the difference in height as long as friction is not active. There is no influence of mass or density. For the case that friction is additionally considered this force acts against flow direction along the flow path.
However, the difference in length of the slopes with different slope angles and a given difference in height and as well the different processing of the computational surface of these slopes is marginal in our case study and would not explain that end velocities decrease with increasing slope angle.
Based on your valuable comment we did further simulations to better analyze the process characteristics we discussed in the manuscript. We could point out that, in addition to the principles in mechanics mentioned above, two basic aspects are relevant for the impact velocities at different slopes:

- In all simulations the difference in heights is equal and already discussed in your comment. However, we did the geometrical set-up in the way that this difference is measured from the sea level to the upper edge of the sliding fluid at the initial position.
  See page 11, line 7.

To maintain the same volume and shape it means that the center of gravity and as well the lower edge of the sliding fluid is at different heights for the different slope situations.
See page 11, line 10.

- The denser fluid does not act as a non-deformable obstacle during the sliding process along the slope. This deformation of the fluid has a substantial influence on the impact velocity.
  See page 13, line 8,9.

We apologize for this imprecise explanation in the manuscript. In the revised manuscript we have firstly described the specific geometrical condition clearer as mentioned here above.
See page 11, line 7,10.

Secondly, we provided a plot showing the temporal distribution of the impact velocity for the sliding fluid for every simulation and compare with assumed values by use of empirical equations and with data from literature.
See figure 6 at page 34.

(20)
Referee:
p12, l7: How can you compare your 3D results with the 2D experimental studies? See also statement p17, l14.

Authors:
We did not use results from previous works to calibrate or rather validate our model output, but just to compare our quality of the results related to the observations with those from other studies, despite the different approach adopted and in order to have a better understanding of the applicability of the modelling approach.
This is done mostly for the model concept analysis.
See section 4.1 at page 12.
See page 22, line 17.

(21)
Referee:
p13: Time intervals refer to time from release, while text all the time describes seconds after impact. This is confusing. What do the x0 values refer to? (also on p14)

Authors:
We refered to the simulation time to make the connection with the images easier, and we used in the text the time from the “impact” to better describe the wave process.
We have considered improvements to make it more consistent.
In the new manuscript we have referred to the denser fluid release to make the link easier with the calculation time steps.
See page 15, line 18,25,35.
See page 16, line 39.
See page 17, line 24.

x_0 is a referred origin coordinate to express the position and the distance of the gauges (history probes). In the impact area it refers to the impact point of the denser fluid at the shoreline. For the whole bay it is located at the shoreline in front of the Cascade Glacier.
See page 12, line 14,16.

In the new manuscript we have shown the location of x_0 in fig. 5.
See figure 5 at page33 .

(22)
Referee:
p13, l17: Is the velocity the same as wave celerity or speed of wave propagation? And if so, how is that quantified?

Authors:
In this work we do not refer to the wave celerity (except for a new additional information in section).
See page 16, line 6.

We refered to the flow velocity, so it is not quantified.
We added more information about the wave propagation starting from the data recorded by the gauges.
See page 17, line 34.
See figure 11 at page 39.

(23)
Referee:
p13, l24: Is flow height relative to terrain? If so, normally referred to as flow depth.

Authors:
Thank you for this note. We have considered this during revising the used terminology in the whole manuscript (see also issues (5) and (9)).
See page 15, line 30,35.

(24)
Referee:
p13, l29: 54 seconds = (34+12+8) seconds from release (not from impact)?

Authors:
Thank for your good attention, this duration is related to the release event. We have corrected this mistake.
See page 15, line 34.

(25)
Referee:
p14, l28: How can the wave slow down due to constriction/narrowing? And why is the wave slower in deeper water? Wave celerity should increase with water depth.

Authors:
Thank you for this note. We have revised the explanation here describing the decrease in “flow velocity” due of the attenuation process of the wave itself where the bay floor increases in depth.
See page 17, line 3.

Concerning the wave propagation velocity, we could actually appreciate a slight acceleration in correspondence of the deepest area of the bay floor.
See page 17, line 40.
See page 18, line 1.

While on the other side (north to the island) the flow velocity is due to a breaking process because of the lower bay floor depth.
See page 17, line 7.

(26)
Referee:
p15, l23: Is the rockslide considered to be a turbidity current?

Authors:
In this section we present the propagation of the sliding fluid on the bay floor as an application available in Flow-3D to observe the mixture process between two fluids with different density, an application that can be adopted also to observe natural phenomena. We agree that is not correct to state that we are observing the propagation of the slide material along the bay floor, but actually a mixture process of the denser fluid approach.
We have clarified this aspect in the manuscript and considered being consistent with terminology.
See page 18, line 21.
See page 21, line 21.

As mentioned in the answer #2, we have considered to be consistent with terminology where the term “rockslide” is used when referring to literature and the description of the observed event. The term “denser fluid” refers to the simplified modelling concept of the current work (see list referring to comment #2)
Additionally, we have decided to skip the (old) figure 13 (denser fluid spreading under water) since it is not relevant for this study (and not physically correct).
See page 50, line 10.

(27)
Referee:
p15, l26: Why is a high-quality reconstruction of the bathymetry more important where the wave characteristics (more used than 'features') change rapidly? l32: And how do you know that a reliable bay configuration has a high influence on model performance and outputs?

Authors:
Thank you very much for this note. We assumed here that it is important to provide high-quality topography and bathymetry in the impact area since this is the location of wave generation. However, it is obviously correct, that with our results this assumption cannot be proven.
We have considered this note during revision of the manuscript in the way that we highlight the general need for appropriate pre-event information of the terrain and, more focusing on the wave features during propagation, especially in areas of lower water depths and interaction with the surrounding terrain.
Additionally, we have decided to skip the (old) figure 13 (denser fluid spreading under water) since it is not relevant for this study (and not physically correct).
See page 18, line 33.
See page 22, line 3.

Further numerical analyses on the influence of the quality of topography and bathymetry are out of scope for the present article.

(28)
Referee:
p15, l36: The results will of course vary with resolution and are normally better with higher resolution (but too high resolution can sometimes also cause instabilities). Again, this is about convergence. See also General Comments above.

Authors:
As previously mentioned, to verify improvements in results in function of the grid resolution, we have provided a conformation of difference reduction and a root mean square error estimate in flow characteristics values, between each refinement.
See page 19, line 32.
See page 20, line 4,8.
See figure 10 at page 37-38.
See figure 13 at page 41.

(29)
Referee:
p15-16: Can some of the results deviating from the general trend be explained by numerical instabilities? E.g. violating the CFL criterion?

Authors:
In all accomplished simulations numerical instabilities or indications for it were not observed. This is of course related to the applied computational meshes. With regard to sensitivity analyses (see issue (3)) simulations with an even finer computational mesh are considered in the revised manuscript and any potentially occurring numerical problems have been discussed.
See page 21, line 3,5.

As far as we know, the CFL-criterion, which is basically important when solving the Saint-Venant-equations (1D and 2D), is not considered in 3D hydrodynamic computations.

(30)
Referee:
p16, l25: A smooth surface? But p11, l6 mentions a sort of a numerical roughness (see comment above).

Authors:
Here we refered to a zero-value for the equivalent grain roughness.
See page 12, line 24,26.

So, for these conditions there is a certain form roughness which is related to the processing of the topography with the FAVOR-method (depending on the size of the mesh cells) present and no further additional roughness.
See page 12, line 20.

We have rephrased this paragraph in order to make it more clear for the reader.

(31)
Referee:
p16, l35: The influence of rockslide characteristics on tsunami genesis is discussed in several papers.

Authors:
We have considered to skip this sentence, since it is not relevant for this study.
See page 20, line 40.

(32)
Referee:
p18, l38: How well suited in hazard analysis is a model that is so computationally costly? Uncertainties are normally treated by running a large number of scenarios.

Authors:
By considering a numerical modelling approach for a very complex topic (multi hazards event) we don´t think that this can be evaluated as computationally highly costly since the simulations finish in terms of days on a “standard” work station (see issue (5) of the authors’ comment to referee#1 for specification) which is in our opinion still acceptable.
See page 23, line 23,27.

So, we support this as a possible approach for hazard analysis (even if it takes longer than valid empirical approaches).
See page 23, line 31.

We fully agree that uncertainties have to be treated by running several scenarios, but this is basically even more relevant on the course of forward-oriented indications (e.g. analysis of potential future hazards) compared to the reconstruction of a historic event where observation data for model calibration is available.

(33)
Referee:
fig. 14: Wave run-up seems to be diverging with mesh refinement. This deserves some discussion.

Authors:
This is explained considering the 3D effect of the topography and considering from which direction the wave approaches and runs upon the topographic surface (from the front in case of section A-A´ and from the side in case of section B-B´).
See page 20, line 8.

(34)
Referee:
I don't think Braathen et al. (2004) is the best single reference for the 1934 Tafjord event.

Authors:
We have included further references in this context, as for instance:

Holmsen, G. (1936): De siste bergskred i Tafjord og Loen, Norge. Svensk geografisk Arbok 1936, Lunds Universitet, Geografiska Institutionen Meddelande, 124, 171-190.

Furseth, A. (1985): Dommedagsfjellet - Tafjord 1934. Gyldendal Norsk Forlag A/S.

See page 25, line 26.
See page 26, line 20.

Lituya Bay 1958 Tsunami – detailedtsunami – pre-event bathymetry reconstruction and 3D-numerical modelling utilizing the CFD software Flow-3D

Andrea Franco[1], Jasper Moernaut[2], Barbara Schneider-Muntau[3], Markus Aufleger[1], Michael Strasser[2], Bernhard Gems[1]

[1]Unit of Hydraulic Engineering, University of Innsbruck, Technikerstraße 13, 6020 Innsbruck, Austria
[2]Institute of Geology, University of Innsbruck, Innrain 52f, 6020 Innsbruck, Austria
[3]Unit of Geotechnical and Tunnel Engineering, University of Innsbruck, Technikerstraße 13, 6020 Innsbruck, Austria

Correspondence: Andrea Franco (andrea.franco@uibk.ac.at)

Abstract. This study aims to test the capacity of Flow-3D regarding the simulation of a rockslide impacting a water body by evaluating the influence of the extent of the computational domain, the grid resolution, the corresponding computation times on the accuracy of modelling results. A detailed analysis of the Lituya Bay tsunami event (1958, Alaska, maximum recorded run-up of 524 m a.s.l.) is presented. A focus is put on the tsunami formation and run-up in the impact area with the numerical model. Several simulations with a simplified bay geometry are performed in order to test the concept of a "denser fluid", compared to the seawater in the bay, for the impacting rockslide material. Further, a topographic and bathymetric surface of the impact area are set up. The observed maximum run-up can be reproduced using a uniform grid resolution of 5 m, where the wave overtops the hill crest facing the slide source, then flows diagonally down the slope. The model is extended along the entire bay to simulate the wave propagation. The tsunami trimline is best reproducedwell recreated when using a) a uniform mesh size of 20 m or b) a non-uniform one of 15x15x10 m with a relative roughness of 2 m for the topographic surface. The trimline mainly results from the primary wave, in some locations also from reflected waves. The "denser fluid" is a suitable, simple concept to recreate a sliding mass impacting a water body, in this case with impact velocities of ~93 ms^{-1}. The tsunami event and the related trimline are well reproduced using the 3D-modelling approach with the density evaluation model available in Flow-3D.

Keywords: Impulse wave, Rockslide, Cascade Hazards, Numerical modelling, Lituya Bay, Mountain hazards.

1 Introduction

The analysis and management of the hydrological and geological risks in mountain regions are considered nowadays as a priority for human and territory safety. Obtaining an accurate understanding of phenomena, like landslides, flash floods and landslide-generated impulse waves, has been and still is a major challenge for reliable natural hazards assessment. In recent decades, the awareness of natural hazard events such as tsunamis in lakes and artificial basins (known as impulse waves) has increased since several disasters occurred (e.g. Tafjord – Norway 1934, Holmsen, 1936, Furseth, 1958, Braathen et al., 2004; Lituya Bay – Alaska 1958, Miller, 1960; Vajont – Italy 1963, Paronuzzi and Bolla, 2012; Chehalis lake – Canada 2007, Wang et al., 2015; Aysen Fjord –

Chile 2007, Sepúlveda et al., 2010; Taan Fjord – Alaska 2015, Haeussler et al., 2018; Karrat Fjord – Greenland 2017, Gauthier et al., 2017). Such tsunamis can be induced by both subaquatic and subaerial landslides (Basu et al., 2010). The creation of new reservoirs for hydroelectric power generation in steep mountain valleys has highlighted the risk evaluation of this type of natural hazard; in particular, the Vajont catastrophe (10 October 1963, Italy) where an enormous landslide collapsed in the reservoir and triggered one of the largest impulse waves ever recorded which killed ~2000 individuals (Paronuzzi and Bolla, 2012).

The generation of impulse waves in lakes or fjords is often caused by a quantity of slope material collapsing and impacting the water body, with enough mass and speed to enable a wave to form and propagate (Basu et al., 2010; Heller et al., 2010; Vasquez, 2017; González-Vida et al., **2019**). These large landslides or rockslides are often triggered by intense rainfall events or earthquakes (e.g. Lituya Bay 1958, Miller, 1960; Chehalis Lake 2007, Wang et al., 2015), evolving in a chain reaction of triggers and consequences.**)**.

The Lituya Bay 1958 tsunami event (Fig. 1) represents a cascading hazard, since an earthquake-generated rockslide (Fig. 2) collapsed and impacted the water body. As a consequence, an impulse wave formed and propagated over a distance of around 12 km to the seaside of the bay and devastated the area surrounding the bay (Miller, 1960). The Lituya Bay case (Fig. 1, 2) marked the beginning of several challenges for the scientific community, where many experts gave their contribution to develop accurate and applicable concepts to simulate and to assess this kind of natural hazard known as landslide-generated impulse wave.

Scientists tried to obtain insights into the **landslide-generated** wave formation due to the rockslide impact in the water body and investigated the characteristics as wave height, amplitude and velocity (Fritz et al., 2001; Mader and Gittings, 2002; Quecedo et al., 2004; Weiss and Wuennemann, 2007; Schwaiger and Higman, 2007; Basu et al., 2010; Chuanqi et al., 2016; Xenakis et al., 2017). The main task was to simulate the rockslide-generated impulse wave and to recreate the observed run-up on the opposite slope adopting different approaches (e.g. physical tests, numerical methods based on Navier-Stokes-equations or Smoothed Particle Hydrodynamics (SPH), see chapter 2.3). A few of them tried to reproduce the phenomena along the whole bay and to give a complete overview and explanation of the event itself (Ward and Day, 2010; González-Vida et al., 2019). **With these studies a significant effort could be achieved in understanding process behavior and hazard potential of landslide-induced tsunamis. The present work also aims to contribute to this. With the focus on the Lituya Bay 1958 tsunami it is addressed to the following research questions:**

Despite many works have been done on landslide-generated impulse waves, many open questions are still present. This work aims to contribute to answer some of these questions:

- Which modelling techniques are available to simulate or reproduce landslide-generated impulse waves?
- Which is the best modelling concept to simulate this kind of phenomena and how high is the requested computational effort to obtain a simulation that adequately reflects the natural processes?
- How far can we go in terms of extent of investigated area and validated results?
- Is a physically correct representation of the landslide collapse and impact process an important factor for the correct representation of wave formation, propagation and run-up?
- What are the role of an appropriate**requirements on** bathymetry and topography reconstruction**in terms of level of detail and accuracy**?
- Can a detailed model help for a better understanding of the whole physical phenomena itself?
- Can we apply knowledge gained from modelling and the concept used for a back analysis to mitigate or prevent such phenomena?

Recently, the most used commercially available software to model impulse waves is the computational fluid dynamics (CFD) model Flow-3D, which is based on a three-dimensional numerical modelling approach (Das et al., 2009; Vasquez, 2017). The objective of this study is to test the capacity and limits of Flow-3D by means of reconstructing a landslide-generated impulse wave on a large spatial scale. An analysis of the past event at Lituya Bay (1958, South Alaska, maximum run-up recorded is 524 m a.s.l.; Miller, 1960, Fig. 1c, 3a) is proposed in this contribution, since a lot of information and data are available for this study and the results can be compared with already existing simulations and publications (e.g. Fritz et al., 2001; Basu et al., 2010; Ward and Day, 2010; Gonzalez-Vida et al., 2019). This deterministic analysis aims to reproduce the tsunami event, using specific data provided by literature, and to validate the modelling results by comparison with the documented tsunami impact. A sensitivity analysis concerning the computational grid resolution and their related outputs is provided.

Since no bathymetry just before the tsunami event is available, a new interpretation of the Lituya Bay and the related shoreline before the event is proposed (Fig. 1, 3), starting from the available cartography and from the free data provided by the National Ocean Service (Hydrographic Survey with Digital Sounding). The pre-event topography is recreated with a resolution of 5 m.

This work focuses on the wave dynamics where a fluid volume moving along the slope represents the trigger process to initiate the wave generation and propagation. Since reproducing the physics (rheology) of the rockslide is not target of this study, the simplified concept of a "denser fluid" in comparison to the seawater is adopted for simulating the impact from the slope. Additionally, the use of a fluid gives the possibility to adapt the volume shape according to the topographic surface during the collapse process.

First, a detailed analysis of the tsunami formation and run-up in the impact area is accomplished with the numerical model. A 3D-model of the impact area (the Gilbert Inlet, Fig. 1c, 2, 4) with a simplified bay geometry as a bucket is reproduced starting from the work done by Basu et al. (2010). Bulk slide volume and density are used to simulate of the observed rockslide, since **are considered for** the concept**set-up** of the "denser fluid", with respect to the water density, is adopted to model the slide material. The presence of the glacier and virtual solid walls to constrain the slide material during the collapse is also considered in the model.**"**. The main task of this part is to test the concept of the "denser fluid" for the impact and to observe wave formation, propagation, and run-up after the impact of the rockslide**denser fluid** into the water body.

In a second step, the Gilbert Inlet is recreated using the real topographic and bathymetric surface. The model is run using three different uniform cell sizes (20-10-5 m). The rockslide**denser fluid** shape is readapted to the detachment area topography. A virtual wall on the right side respect the rockslide body is set to constrain the material during the collapse.

Moreover, the model is enlarged to simulate the propagation of the wave along the entire bay (Fig. 5) and to recreate the inundated area and the related trimline. The results change in function of the cells size adopted for the simulation (20x20x20 m, 20x20x10 m, 15x15x10 m). An analysis concerning the adoption of different roughness values for the topographic surface (relative roughness: 0-1-2 m) is accomplished with the numerical model. The propagation of the rockslide material along the bay floor can be observed using the second order approach for the density evaluation.

2 Study case

2.1 Geomorphological and tectonic setting of Lituya Bay

Lituya Bay is a fjord in southeast Alaska, originated by the glaciers retreat (Fig. 1a) ten thousand years ago at the beginning of the current interglacial period (Pararas-Carayannis, 1999), resulting in its present T-shape (Fig. 1b). U-shaped slopes are the main features of the bay, with recent terminal moraine deposits of former Tertiary glaciation periods (Pararas-Carayannis, 1999).

At the head of the bay the slopes exhibit very steep walls, from 670 to 1030 m a.s.l. and to more than 1800 m a.s.l. in the Fairweather fault area, about 3 km from the Crillon Inlet. **The Lituya Bay has a length of 12 km and its width ranges from 1.2 to 3.3 km (Fig.** 1b), while the entrance is about 300 m wide (Fritz et al., 2001). **The northern and southern channels on the side respect Cenotaph Island in the middle of the bay are about 650 and 1300 m wide (Fig.** 1b). The shores consist mostly of rocky beaches. At the entrance of the bay, La Chaussee Spit (Fig. **1b) represents the terminal moraine resulting** from the Last Glacial Period (Pararas-Carayannis, 1999).

The Queen Charlotte and Fairweather Faults are situated at the west coasts of Canada and Alaska north to Lituya Bay. They are part of the fault system along the boundaries of the Pacific and the North American plate (Tocher and Miller, 1959). The Gilbert and Crillon Inlet represent the geomorphological expression of the Fairweather Fault.

2.2 The Lituya Bay 1958 tsunami event

Fritz et al. (2001) report that in the last two centuries in Lituya Bay**from 1980-2000** four (probably more) big waves could have been verified in Lituya Bay. This occurrence is most likely due to the "unique geologic and tectonic setting of the bay

" (Fritz et al., 2001). Miller (1960) reports that several tsunami events happened in Lituya Bay (1853, 1936 and 1958), devastating the forest and reaching a run-up of over 100 m a.s.l. in the inland.

Compared to many other bays or fjords, the numerous manifestations of tsunami in the Lituya bay are due to several factors. These are a) its recent environment history (a fjord formed by glacier retreat), b) the fragile geological and tectonic configuration (steep slopes consisting of fractured rock slopes in a very active fault area), c) the presence of a great amount of water in the bay and a deep seafloor, and d) its climate condition including intense rain events and periodic freezing and thawing (Miller, 1960).

The earthquake from July 9, 1958, featuring a 7.9-8.3 Richter magnitude, occurred along the Fairweather fault. A rockslide collapsed into the bay, at the Gilbert Inlet (Fig. 1) (Fritz et al., 2001). Horizontal movements of 6.4 m and vertical movements of 1.0 m were estimated for the earthquake as reported in Tocher and Miller (1959). Fishermen that experienced the event spoke about 1 to 4 minutes of shaking. The earthquake may have triggered the rockslide owing to powerful seismic ground movement (Fritz et al., 2009). The impact of the rockslide generated a huge impulse wave whose maximum run-up (524 m a.s.l., Fig. 1c, 2b) is the highest ever recorded in history (Fritz et al., 2001). The wave propagation along the bay resulted in forest destruction and ground erosion (Fig. 1b). Miller (1960) hypothesizes the rockslide as a source of the tsunami evaluating photographs from the slopes at the Gilbert Inlet before and after the event. He estimates the volume of the main rockslide ($30x10^6$ m^3) and defined the upper scar limit at about 915 m a.s.l. (Fig. 1c, 2a).

To be able to distinguish this mass movement from gradual processes and ordinary landslides, Pararas Carayannis (1999) classify it as "subaerial rockfall", while Miller (1960) describes it as a mixture between a landslide and a rockfall process according to Sharpe (1938) and Varnes (1958).

Before the catastrophic event, two gravel deltas were located in front of the Gilbert Glacier (Fig. 1b,c). The rockslide propagated with very high speed (Ward and Day, 2010), hitting a part of the glacier and the gravel deltas (Miller, 1960). After the event, the glacier front showed a vertical wall (Fig. 2a), since 400 m of ice have been disintegrated and the collapsed **deltas**. The rockslide triggered a huge impulse wave that reached a run-up of 524 m a.s.l at maximum. (Fig.1c, 3a) on the southwest slope of Gilbert Inlet (Fritz et al., 2001). This is the maximum run-up ever recorded in history. Ward and Day (2010) describe the water ran upslope as a surge or splash. The second maximum run-up of 208 m a.s.l. has been identified near Mudslide Creek on the southeast side of the Gilbert Inlet (Fig. 1b). The wave reached a distance in the inner land of 1400 m on the plain in front of Fish Lake (Fig. 1b) on the northwest side of the bay (Ward and Day, 2010).

Two fishermen eyewitnessed shortly after the first shaking **eye-witnessed** a violent disturbance at the mouth of Gilbert **shortly after the first shaking** and confirmed the rockslide as trigger of the impulse wave (Ward and Day, 2010). The fishermen estimated the wave's amplitude to be about 15-30 m as it impacted the Cenotaph Island (Fig. 1b). Additionally, they experienced, at their boats, a short period with wave heights up to a few meters shortly after the initial wave (Ward and Day, 2010).

2.3 Existing studies on the Lituya Bay 1958 Tsunami event

As one of the most studied cases for landslide-generated impulse waves, the Lituya Bay Tsunami 1958 has been and still is of great interest for the scientific community concerning the assessment of natural hazards. Different approaches have been used to reproduce the tsunami like**covering analytical studies,** physical scale tests, empirical studies and numerical modelling.

2.3.1 Physical scale tests

A three-dimensional model of Lituya Bay at a 1:1,000 scale was created by Wiegel (1964). Thereby, a run-up of about three times of water depth was observed on the opposite slope of the sliding source. Additionally, a second high run-up has been observed close to the Mudslide Creek area, while the wave was propagating along the bay. Moreover, Wiegel (1964) estimated the hydrodynamic forces of the wave which impacted the trees as about ten times higher than the force needed to chop the trees.

. Fritz et al. (2001) recreated the Lituya Bay 1958 tsunami in the impact area. He simulated the wave formation and run-up in a two-dimensional physical scale model as a vertical-section of Gilbert Inlet at 1:675 scale at ETH Zurich (Laboratory of Hydraulics, Hydrology and Glaciology). In order to recreate a high-velocity granular slide and to control the impact process in to the waterbody, a landslide generator with a pneumatic mode was applied.**.** The results confirm the hypothesis of the rockslide as a high possible source of the impulse wave and the related**observed** maximum run-up of 524 m a.s.l. **. A three-dimensional pneumatic generator for landslide-generated impulse waves was applied by Fritz et al. (2009). The Lituya Bay 1958 rockslide was thereby recreated in a three-dimensional model at a scale of 1:400.**

A three-dimensional pneumatic generator for landslide-generated impulse waves has been tested in a wave basin at Oregon State University) (Fritz et al., 2009). The Lituya Bay 1958 rockslide has been recreated in a three-dimensional laboratory model at a scale of 1:400.

2.3.2 Empirical

The equation applied by Fritz et al. (2004) for the maximum wave height a.s.l. gives the measured **A number of studieis based on the application of analytical equations, amongst derived from experimental analyses. With it,** amplitude of 155 m. Kamphuis and Bowering (1970) obtained from their experiments a measured wave height of 162 m. The linear wave theory to produce wave formation and motion has been adopted by Noda (1970) assuming a body collapsing vertically into a basin. The results obtained from this theoretical solution underestimate**the impulse wave as well as maximum run-up were reconstructed. Concerning** the maximum wave amplitude with 122 m by 20 % with respect to Fritz et al. (2001). **impulse wave height, obtained results are within the range 94-162 m (Kamphuis and Bowering, 1970; Noda, 1970;** Slingerland and Voight (**,** 1979) overestimate the observed wave height resulted from an empirical regression obtained from two case studies.**;** Huber and Hager (**,** 1997) defined an empirical formula to estimate two-dimensional impulse wave features and they calculated a wave height of 94 m. Noda (1970) as well as Kamphuis and Bowering (1970) tested a sliding block as a source for the wave formation. As confirmed by Fritz et al. (2009), they observed a high influence of the slide impact thickness and the slide Froude number on the wave features.

; Fritz et al., 2004; Fritz et al., 2009). Hall and Watts (1953) and Synolakis (1987) matched the Lituya bay 1958 maximum run-up respectively of 526 m a.s.l. and 493 m a.s.l adopting solutions for solitary wave run-up, considering an impermeable slope and**.,** assuming the measured impacting wave height of 162 m and **a water depth of -**122 m as input (Fritz et al., 2001). Their results support the experiments of Slingerland and Voight (1979), where back-calculation of wave height from run-up confirms **) confirmed** that a wave crest**height** of about 160 m is required to recreate the maximum observed wave run-up.

Heller and Hager (2010) applied the impulse product parameter to estimate the landslide-generated impulse wave main characteristics in Lituya Bay. Considering a slide impact velocity of 92 ms^{-1} (Körner, 1976), they predicted a wave height of 179 m based on the wave channel geometry.

2.3.3 Numerical modelling

Starting from the experiment of Fritz et al. (2001), Mader and Gittings (2002), Quecedo et al. (2004), Weiss and Wuennemann (2007), and as well Basu et al. (2010) numerically simulated the Lituya Bay 1958 tsunami event with a focus on the impact area by applying the Navier-Stokes hydrodynamic code in two dimensions. Mader (2001) applied the SWAN-code (Simulating Wave Nearshore) to numerically model distinct feasible wave trigger mechanisms. The code solves the non-linear long wave equations. These studies stated that a straightforward landslide-generated tsunami leads to wave floods. If the slide would lift a volume of water equal to the slide volume upon the sea level, it results in less than one tenth of the observed one. Mader and Gittings (2002) simulated the Lituya Bay tsunami with the full Navier-Stokes AMR Eulerian compressible hydrodynamic code (SAGE). With it, the maximum wave height was 250 m. It ran up to 580 m a.s.l. at the opposite slope, being comparable to the observed 524 m a.s.l.

Pastor et al. (2008) applied a coupling model in displacement and pore pressure together with an appropriate**a** generalized plasticity model that describes soil behavior. Propagation is evaluated using a depth-integrated model with fluidized soil rheology. The third stage – slide**Slide** and water interaction – is simulated with a level-set algorithm that tracks the interfaces between air, water and solid. They computed a maximum wave height of 226 m for a slide impact velocity of 110 ms^{-1}.

leading to a maximum wave height of 226 m. To simulate the tsunami run-up, Weiss et al. (2009) used a hybrid model approach for the movement of deformable bodies in a U-shaped valley (comparable to the Gilbert Inlet). They obtained a maximum wave heightamplitude of 152 m and a maximum run-up of 518 m a.s.l.

Basu et al. (2010) applied the drift-flux model implemented in the CFD software Flow-3D to simulate the landslide-generated impulse wave formation in the impact area of Lituya Bay. Assuming an initial void fraction of 40 % for the rockslide material they predicted a maximum amplitude of 200 m and a maximum run-up height of around 673 m a.s.l.

The two-dimensional representation of Lituya Bay according Fritz et al. (2001) was also used in the context of a SPH (smoothed particle hydrodynamics) modelling approach by Schwaiger and Higman (2007), Chunqi et al. (2016) and Xenakis et al. (2017). SPH allows a better representation and simulation of the landslide material collapse process and its impact into the water body.

Accurate numerical models of the Lituya Bay 1958 Tsunami event with a detailed reproduction of the bathymetry and the surrounded topography are scarce (Ward and Day, 2010; Gonzalez-Vida et al., 2019). Ward and Day (2010) developed a new "tsunami ball approach" to simulate the impulse wave formation and propagation along the whole Lituya Bay. As they describe, "this approach uses a momentum equation to accelerate bits or balls of water over variable depth topography, where the thickness of the water column at any point equals the volume density of balls there". They predicted a wave height up to 150 m in the impact area and a run-up height of 500 m .a.s.l. For their final simulation, theyThey considered a dual source for the tsunami event: the subaerial rockslide and a huge amount of subglacial sediments released in the bay after the rockslide impact in the water body. The resulted trimline is overestimated by the dual source approach, but only the subaerial rockslide as impulse wave trigger was not enough to explain the whole flooded area along the bay.

Gonzalez-Vida et al. (2019) modelled the Lituya bay tsunami event withapplied a finite volume Savage-Hutter Shallow Water coupled numerical model (HySEA). The resulting numerical simulations succeeded in reproducing most of the features of the tsunami event.

3 Methods, data and model set-up

3.1 Pre-event bathymetry and topography

Digital data and cartographic material concerning the bathymetry and topography of Lituya Bay, dated before and after the tsunami event, are available. None of these data is closed enough to describe the exact configuration of the bay shortly before 9 July 1958.

The 1926 and 1940 bathymetry surveys (U.S. Coast and Geodesic Survey, 1942) show that the northeast limit of Lituya Bay has a U-shaped valley with steep slopes and a wide flat sea bottom, increasing constantly its depth until the maximum point of -220 m a.s.l. on the southern side respect to Cenotaph Island (Pararas-Carayannis, 1999), then decreasing in direction of the sea. In the area close to the bay entrance, the bay floor is at - 10 m a.s.l. in average. The observed bay floor configuration suggests high sedimentation rates in time. However, information about the sediment deposit thickness is not available (Pararas-Carayannis, 1999).

Miller (1960) has been the first after 1958 who described the bay before the tsunami event (Fig. 1c). He describes the area between Cenotaph Island and Gilbert Inlet as a wide expanse with depths between -150 and -220 m a.s.l. He highlights the presence of two deltas on both sides in front of Gilbert Inlet. In the maps reported in Fig. 4a,b Miller (1960) mapped the topographic and the bathymetric contours pre-event. In the post-1958 surveys, these areas and deltas are not present (Ward and Day, 2010). The 1969 chart obtained from the 1959 survey (U.S. Coast and Geodetic Survey, 1969) shows a flat sea bed (green zones in Fig. 4a). A ridge divided the bay floor into two sub basins: a smaller one southeastern respect to the Gilbert Head (-156 m maximum depth), and a larger on south front of Cenotaph Island (-150 m maximum depth).Ward and Day (2010) estimated that 3 x 10^8 m^3 of material discharged into the bay, filling it until the 130 m depth contour, resulting in a 70 m thick deposit. A third survey published in 1990 (U.S. Coast and Geodetic Survey, 1990) gives the possibility to estimate the sedimentation rate in time. The two charts, first from 1942 to 1969 and second from 1969 to 1990, differ completely. Indeed, the **(see Figure 8 in Ward and Day, 2010).** The north-eastern sub basin in front of the Gilbert glacier is filled by sediments. **The** bay floor decreases constantly between the Gilbert Inlet and the basin in front of Cenotaph Island. From these considerations, Ward and Day (2010)**Ward and Day (2010) estimated that 3 x 10^8 m^3 of total material discharged into the bay after the tsunami event, filling it until the -130 m depth contour, resulting in a 70 m thick deposit. From the previous considerations, they** propose a hypothesis to justify the whole infill of the bay between 1926 and the 1958 tsunami event. Given that: i) the sedimentation rate is assumed constant during the last century; ii) in 1936 a landslide collapsed in the bay (where the generated wave was 1/10 the size of the 1958 tsunami,; Miller, 1960); iii) the 1958 rockslide contained 3-6 x 10^7 m^3 of material (10-20 % of the total infill volume), and iv) soil, sub soil and bedrock have been eroded by the wave (about 4 x 10^6 m^3, Miller, 1960); they suggested that the **remobilized** sediment located under the displaced Gilbert Glacier body during the tsunami event contributed to infill the bay for the volume that they have estimated, and so contributed to the impulse wave propagation.**floor during the tsunami event.** The possible volume generated from the displacement of the deltas in front of the Gilbert Glacier has not been considered as a possible source of material to justify the whole infill in the bay after 1958..

All these considerations are useful to give a good interpretation of the bay pre-event configuration (Fig. 4c). The bathymetric and topographic surfaces have been recreated with the 3D-design model Rhinoceros 6 (https://www.rhino3d.com/), using the command Patch that fits a surface through selected curves, meshes, point objects, and point clouds.

3b). The bathymetric data used for this study is provided by the National Ocean Service: Hydrographic Surveys with Digital Sounding. In particular, data from Survey ID: H08492, 1959, is used as reference bathymetry after the event since this survey is the closest to the 9 July 1958 tsunami event, and data from Survey ID: H04608, 1926, the closest previous to the event. The survey from 1926 has not enough resolution to provide an acceptable bathymetry in the whole bay. Nevertheless, it provides sufficient information of the pre-tsunami bathymetry in the areas at Gilbert Inlet and south to Cenotaph Island. As mentioned in Ward and Day (2010), the infilling material after the 1958 event covers an area that remains under the -120 – -130 m depth contours. In the map (Fig. 4a) that area includes the, contour lines defined by Miller (1960) **(red dashed lines in Fig. 3a)** from a depth of -122 m to -220 m. **show the bay bathymetry before the infill.** From these considerations, the elevation points from the Survey ID: H08492, 1959, are taken as representative of the shallower part of the bay floor (from the surface to -120 m depth). Below -120 m depth, the elevation points from the Survey ID: H04608, 1926, are considered to be representative of the deeper area of the bay floor. Due to few data, the contour lines defined by Miller (1960) are used to better reproduce the shape of the bay floor. In addition, for flatter parts, lines are set between different elevations points to allow a more accurate interpolation for the bay floor surface reconstruction. The delta in front of the Gilbert Glacier (Fig. 3a) is reproduced considering the information given by Miller (1960).

The topographic surface pre-event is reproduced starting from the current digital terrain model (5 m resolution) available from the DGGS Elevation Portal of Alaska. Contour lines of 5 m are used to recreate the topography.

Where necessary, contour lines of 1 m are also used to highlight some details that influence the estimation of the flooded area (as steeper slopes, hills or specific curves). The observed trimline and the run-up records (red spots in Fig. 3b) are used as references to define the required spatial extent of the model topography.

Additionally, the**Manual modifications of the DTM are provided at the Gilbert and Crillon Inlet locations in order to recreate those geomorphological elements that have been displaced and washed away during the landslide impact and wave formation. The** Gilbert Glacier body is recreated starting from the descriptions provided by Miller (1960) and the available cartography (Fig. 4b**see Figure 16 in Miller, 1960**), so the shape of the two deltas located in front of the glacier. **The same is done for the Crillon Inlet.** Miller (1960) describes a scars area located northern of the maximum observed run-up as pre-existent the tsunami event (Fig. 2b, Pre-1958 Landslide scars). He reports only a little scar exactly under the maximum run-up (524 m a.s.l.) that could be eroded from**form after** the wave**tsunami event**. Also the pre-event shoreline is reproduced starting from the descriptions provided by Miller (1960).

The bathymetric and topographic surfaces are recreated and exported to stereolithography files (stl) by use of the software Rhinoceros 6 (https://www.rhino3d.com/).

3.2 Model setup and computational details

3.2.1 Solver methodology

For computational modelling the CFD software Flow-3D (Harlow and Welch, 1965; Welch et al., 1966; Hirt and Nichols, 1981; Flow Science Inc., 2018) is applied. Its solver is based on a finite volume formulation in an Eulerian framework. The partial differential equations express the conservation of mass, momentum, and energy of the fluid in the computational domain. The software enables the possibility to simulate two-fluid problems, incompressible and compressible flows, and as well flow conditions at highly different Reynolds-numbers (laminar, turbulent). Flow-3D solves the Reynolds-averaged Navier-Stokes equations (RANS) adopting the Fractional Area/Volume Obstacle Representation (FAVOR) (Hirt and Sicilian, 1985) and the Volume of Fluid (VOF) (Hirt and Nichols, 1981) method.

The Reynolds-averaged Navier-Stokes and the continuity equations are expressed as follows (Hinze, 1975):

$$\frac{\partial \bar{u}_i}{\partial t} + \bar{u}_j \frac{\partial \bar{u}_i}{\partial x_j} = -\frac{\partial p}{\partial x_i} + \mathrm{v}\frac{\partial^2 \bar{u}_i}{\partial x_i\, \partial x_j} - \frac{\partial \mathrm{T}_{ij}}{\partial x_j} \quad \text{for} \quad \mathrm{T}_{ij} = \overline{u_i' u_j'} \qquad (1)$$

$$\frac{\partial \bar{u}_i}{\partial x_i} = 0 \qquad (2)$$

where $\bar{u}$ is the Reynolds-averaged fluid velocity, p is the Reynolds-averaged pressure (divided by the density ρ), ν is the kinematic viscosity of the fluid and T is the Reynolds-stress term (which include the reaction of the turbulent motion on the mean stresses) (Hinze, 1975).

The VOF method is a two-phase solution where the grid includes both the water and air. With this approach every cell in the mesh has a fraction of water (F), which is equal to 1 when the cell is fully water-filled and 0 when it is air-filled. In a case between 0 and 1, the cell comprises the free water surface. A transport equation is thus considered as follows (Rady, 2011):

$$\frac{\partial F}{\partial t} + u\frac{\partial F}{\partial x} v + \frac{\partial F}{\partial y} + w\frac{\partial F}{\partial z} = 0 \qquad (3)$$

where u, v and w are the components of the fluid velocity u in x-, y- and z-direction.

The FAVOR-algorithm (Hirt and Sicilian, 1985) permits the definition of solids within the orthogonal computational grid and computes areal and volumetric fractions of blocked volumes of each computational element. A set of turbulence models is implemented in order to cope with the problem in context of the RANS-equations and to simulate turbulent flow conditions respectively. For this work, the RNG-model (Yakhot and Smith, 1992) is used. It adopts statistical models to calculate the two model parameters, the turbulent kinetic energy and the turbulent kinetic energy dissipation rate.

Several tools and parameter modules are useful to simulate a body sliding along a slope and impacting a water basin, depending on which kind of gravitation process is going to be simulated (rockfall, rockslide, rock avalanche or snow avalanche). To use a denser fluid, in respect to the seawater density, for the sliding mass is a suitable concept for those gravitational processes that behave more like a fluid during their collapse and run-out process. That's the case of the Lituya Bay 1958 rockslide (evolved into a rock avalanche).**The use of this solution to qualitatively recreate the sliding process (similar to the model described by Miller, 1960 and Fritz et al., 2001) is a well suited approximation for the impact modelling of the Lituya Bay event.** Both the first and the second order approaches for the density evaluation implemented in Flow-3D are adopted to simulate the two fluids and their interaction, also in order to understand which one is suitable to perform better the rockslide material.**.** These models (first or second order) compute**calculate** a separate **distinct density** transport equation for the density and simulate**perform** the movement**motion** of two different fluids (of different densities) in the domain. In this way,**, thereby simulating** two fluids can be simulated along**together** with a free surface (Flow- 3D, **Science Inc.,** 2018).

All simulations are run with the same computation resource with the following hardware components:

- **Processor: Intel® Core™ i7-3820 CPU 3.60 GHz,**
- **RAM: 32 GB,**
- **System type: 64-bit Operating System,**
- **Graphic card: GeForce GTX 6602 (Integrated RAMDAC, total available memory 4096 MB),**
- **Number of core license tokens checked out: 8 (Flow-3D parallel license code).**

3.2.2 RockslideDenser fluid setup

The cliff material consists mostly in amphibole and biotite schists with an estimated density of the undisturbed rock of 2700 kgm^{-3} (Table 1). The sliding mass dimension before the collapse is well known. The thickness of the slide has been defined by Miller (1960). The mass of the rockslide is described as a rock prism with a triangular shape (along a vertical section) with a width varying from 730 m to 915 m (Miller, 1960; Slingerland and Voight, 1979; Fig. 1c). The length results in 970 m along the slope (Slingerland and Voight, 1979, Table 1). The maximum thickness results in 92 m; the center of gravity is located at 610 m elevation (Miller, 1960; Table 1, Fig. 1c). Miller estimated the volume of the sliding mass to be about 30.6 x 10^{6} m^{3} with an elevation from 230 to 915 m a.s.l. Since the concept of a denser fluid is adopted, a bulk slide volume and a bulk slide density, respectively 51.0 x 10^{6} m^{3} and 1620 kgm^{-3}, are used for the denser fluid simulation (Table 1). As done in Fritz et al. (2001), the reduced bulk density of 1620 kgm^{-3} considers a void content of n=40 % (Table 1). The used porosity is based on data from debris flows observed in the Alpine Region (Tognacca, 1999). This is not entirely representative of the real rockslide material. However, this assumption is related to the denser fluid concept where the slide collapses with the behavior of a fluid **but gives an appropriated approximation for the trigger mechanism of the landslide-generated impulse wave**.

3.2.3 SimplifiedModel concept analysis

An idealized 3D model of the Lituya Bay topography as a bucket shape is assumed for the model concept analysis (Fig. 4a), starting from the information provided by the 2D-numerical simulations proposed by Basu et al. (2010) that resume the experiment of Fritz et al. (2001). The simulation time is set to 60 seconds. Terrain model and as well the computational domain are presented in Fig. 4a.

Different slope angles of 35-40-45 degrees are set to verify the influence of the impact angle on the impact velocity (Fig. 4b). Despite the change in inclination, in all simulations the difference in heights is maintained equal, thus the geometrical set-up is done in the way that this difference is measured from the sea level to the upper edge (915 m a.s.l.) of the denser fluid at the initial position (Fig. 4b). 5. **To ensure the same volume and shape, the center of gravity (as well as the lower edge of the denser fluid) is at different heights for different slope situations.**

The computation domain extends 3187 x 2225 m and is 1122 m in elevation, where 0 is**has its origin** located at the bay floor, assumed to be -122 m from**below** the sea level (Fig. 5, Table 2). A non-uniform **An** orthogonal grid comprising a mesh of 250 x 250 x 140 **uniform** cells (respectively for the x, y, z axes, Fig. 5, Table 2) is **size of 10 m is** defined for these models. The grid includes the air space above the bay between the headlands to accommodate the waves according the VOF-algorithm (Basu et al., 2010).

The boundaries are specified as outflow on the free sides of the idealized topography to allow the fluid to flow out of the model without any kind of interaction or reflection. The extent of the flow domain is set in the way that the fluid interacts mostly with the boundary that represents the bay floor and inland slopes (left and right boundaries). To save memory and best possibly decrease calculation time, a solid body is set up in the air space occupying most of the cells that are supposed to be not involved in the calculation since the wave would not reach them (the same concept is adopted for all simulations in the impact area and the entire bay). An idealized 3D rockslide body is defined (Fig. 5), featuring a thickness of 92 m as done by Basu et al (2010). Most of the mass is concentrated in the upper part of the rockslide with the purpose to get enough velocity during the collapse process and the impact in the water body (Fig. 5, 7a).

The presence of the glacier and solid**possible virtual** walls to constrain the slide material **fluid** during **its movement along** the **slope** is also taken into account in both simplified and the impact area simulation**considered** (Fig. **4a). With regard to the evaluation of** the modmodelling concept, it is expected that the impact velocities stay within the interval 90-110 ms^{-1} (Table 2).

The initial fluid in the bay represents typical seawater conditions and features a density of 1035 kgm^{-3} (Table 1).

3.2.3 Models description

3.2.3 Modelling of the impact area and the whole bay

Further simulations in the impact area included the topography surface and the recreated bathymetry (Fig. 5, Table 2). The simulation time is 70 seconds. Different uniform cell sizes are set up for these simulations (20 m, 10 m and 5 m) in order to verify the accuracy of the results in function of the grid resolution (Table 2). The simulation domain extends 1600 x 4000 m in X - Y direction and 1200 m in elevation. The same boundary conditions as used for the simplified analyses**model concept analysis** are set for these simulations. The rockslide**denser fluid** shape is redefined starting from satellite images and cartographic material pre-event. The resulting volume is readapted to the detachment area. The maximum used slide thickness of 134 m is equivalent to 1.4 times the thickness of 92 m provided by Miller (1960). This increase of 40 % in thickness was considered also by Fritz et al. (2001). They adopted this rise in slide density to compensate for the void fraction current in granular flow to match the slide mass-flux per unit width. The same concept has been assumed for the fluid mass in this part of the work.

For the impulse wave propagation along the whole bay, the domain extends 6810 x 13575 m in X - Y direction and 1200 m in elevation (Fig. 5, Table 2). The simulation takes a time of 7 minutes. Uniform and non-uniform cells of different size are set up (20x20x20 m, 20x20x10 m and 15x15x10 m). At the domain limits at Gilbert and Crillon Inlets and at the seaside, the outflow boundary condition is set to allow the wave to flow out from the model domain.

Control points (Fig. 5) representing specific records of run-up are set in order to validate the results. Several observation gauges (history probes) are set along the entire model domain to achieve information regarding the slide shape, impact time, impact velocity, wave features**propagation speed and characteristics** as wave height**water surface elevation** (or wave amplitude), wave**flow** velocity **magnitude (total velocity considering all the vector components)** and their trend in time. In the impact area, probes P1-P2-P3 are located along the main wave flow direction (Fig. 5), for a distance x_o of 45-688-1342 m respectively from the slide impact point. Other history probes are set parallel to the bay length (Fig. 6), starting in front of the delta in correspondence of the Cascade Glacier for a distance x_o of 600 m (P4), 3100 m (P5), 5600 m (P6), 6600 m (P7N/P7S, both located laterally respect Cenotaph Island), 8100 m (P8) and 10600 m (P9).

The surface roughness in Flow-3D consists of two components: The first results from the preprocessing phase of the considered solid structures (stl-files) with the FAVOR-method. Depending on the mesh structure and resolution it features divergences from the original solid structure. The computational geometry usually features a rougher surface than the solid structure in the case that the mesh orientation does not fit perfectly with the surface slope. Furthermore, an additional roughness parameter, defined as equivalent grain roughness (m), can be set for each solid structure to consider for example vegetation.

The computations in this study are set-up mainly with **an almost** smooth surface for the topography (zero relative roughness). The actual solid surface where the computation occurs is redefined by the computation **topographic surface (equal to 0 m in additional equivalent grain roughness). In order to verify the influence of the vegetation on the inundation process and the trimline definition, simulations with values of 1 m and 2 m are set up for simulations with a** grid. The regenerated surface has a sort of roughness that can be representative of the actual topography roughness itself **resolution of 15x15x10 m**.

4 Results

4.1 Evaluation of the rockslide**denser fluid** concept

Several preliminary simplified simulations are accomplished with the numerical model in order to test the concept of the "denser fluid" in respect to the seawater density for the rockslide material. Different slope angles of 35-40-45 degrees are chosen to verify the influence of the impact angle on the slide impact velocity.**impacting fluid.** Different configurations are investigated: **a) different slope angles (35-40-45 degrees), b)** absence or presence of the Gilbert Glacier (as a vertical wall of 100 m a.s.l.**), and c)** use of **virtual** walls to constrain the slide material**denser fluid** during its collapse process.**movement along the slope.** This is done to observe the reaction of the wave in dependence of the changes in these options in comparison to the simple bucket shape.

The whole process reflects what resulted from the experiment of Fritz et al. (2001), where they describe the high velocity of the slide impact process with the following two main steps: a) the impact of the slide, with the emergence of cavity effects and generation of the impulse wave, and b) the collapse of cavity effects and components mixing phase processes. The formation of a large air cavity after the initial impact is well observed in the computational model.

Several observations on these **The** results **of the model concept analysis** are discussed in **this context in** the following.**:**

- The rockslide**denser fluid** reaches the water body in a time between 11-13**within 10-14** seconds with a**. Maximum** velocity varies in a range 93-104**between 92-114** ms^{-1} as a function of the **modelled** impact angle (slower for 45° and faster for 35°). This can be explained since setting**Fig. 6c). Since** the rockslide **denser fluid does not act as a non-deformable body during** the **moving process along the slope** same altitude, for a constant slope angle, it varies lightly the slope length (longer for 35°, less for 45°) and the distance that the rockslide takes to run until the waterbody. Ignoring friction, longer distances allow the slide more time to get higher speed at**, also its center of gravity changes position during movement. This fluid deformation has a considerable influence on** the impact. **velocity. In Figure 6 the fluid velocity during the impact process is shown for every considered slope angle. An upper and lower limit (dashed black lines) define a reasonable velocity interval for the center of gravity hitting the water body (values obtained from the equation 3.1 provided by Heller et al., 2009, with a dynamic bed friction angle δ of 0 and 14 degrees).**
- The presence of one or two walls**virtual** constraining the rockslide material**wall** does not significantly influence the rockslide**impact** velocity, while it avoids the slide material**mass** to spread along the slope during its collapse process.**movement.**
- The impulse wave is formed and reaches its maximum height after 8-11**9-10** seconds from the impact, with a wave height**amplitude** ranging between 177-223**203-220** m.
- The presence of the glacier does not influence the wave formation, while the presence of the constraining walls increases the wave amplitude of 10**5** to 40**15** m. This means that the rockslide shape of the **denser fluid (fluid** thickness)**), as it is constrained by the walls** at the impact**,** influences the wave features**characteristics** more than the impact velocity. **The presence of the glacier does not influence the wave formation.**
- The additional presence of the glacier, together with the constraining walls, affects and increases the impulse wave just before the impact on the opposite headland (18-20 seconds after the slide impact). Here the wave height**amplitude** ranges between 136**156** and 214**217** m. It is observed that the wave has no possibility to complete its breaking process, hitting very violently the opposite headland and starting its run-up process along the slope.
- Different maximum run-up values result for the different model configurations. They range**overestimate the observed one, ranging** from 463**570** to 700**790** m a.s.l. between 31-35**36-38** seconds after the slide impact and 12**16**-17 seconds after the wave hits the opposite headland. Once the maximum run-up is reached, a backflow of the wave is observed.
- Most of results are close to the maximum recorded**Closer** run-up **(values to** 524 m a.s.l.**)**. **are found** for calculations considering the simple bucket shape of the bay, without the presence of the glacier and walls. Results considering the glacier and the walls mostly overestimate the maximum observed run-up. This means that the model, as it has been conceived, reflects in a quite reliable way the experiments and the numerical simulation proposed by Fritz et al. (2001) and Basu et al. (2010), and the results are in good

agreement with these previous works. **Considering these two elements in the model, the maximum observed run-up is highly overestimated.**

- It is noticed that the use of different order approaches for the density evaluation influences the rockslide material behavior during its run-out process into the water body along the bay bed.**interaction between the two fluids.** With the first order approach, a**the** mixing process between the two fluids (the rockslide material and the sea water) takes place; most of the slide material is dispersed in the sea water, changing**leads to a change** in density (**of the denser fluid** from 1620 to about 1350**1250** kgm^{-3}). On the contrary, with**. With** the second order approach, the slide material density is mostly maintained until the end of the simulation (60 seconds), where a mixture happens in front and on the upper side of the rockslide body.**changes to 1400 kgm^{-3}.** In both cases, a part of the rockslide material**denser fluid** runs up a short distance on the opposite headland for an elevation almost equal to the water depth.**slope.** The influence of the use of one approach or the other on **does not influence** the wave **characteristics** features is still not clear.

The main task of several authors was to reproduce the impulse wave formation and reach the observed run-up. Once the wave run-up could reproduce this value and flows back, it was supposed to have obtained a reliable result and a good reproduction of the Lituya Bay 1958 tsunami event. However, this is not properly correct if the complete run-up process is taken into account. The wave actually did not stop at 524 m a.s.l. and flow back (only), but overtopped the hillcrest and continued to flow diagonally along the slope to the other side for a distance of about 1 km before reimpacting the sea (Fig. 1c, 3a). This means a wave that reaches “only” a run-up of 524 m a.s.l. and flows back is not enough to reproduce what actually happened that day in Lituya Bay at Gilbert Inlet. More "power" is needed to reproduce the phenomena and what has been observed not only in the impact area but in the whole bay. For the model concept, the presence of the glacier and walls to constrain the slide material during the collapse are necessary to recreate the impulse wave formation and run-up at the head of Lituya Bay, where an**re-impacting the sea (Fig. 1c, 2b). An** overestimation of the maximum run-up, in these simplified simulations, makes sense to allow the further overtopping at the **hillcrest. More "power" is needed to reproduce the phenomena and what has been observed in the whole bay and in the impact area. For the model concept with a topographic surface, the presence of the glacier (and walls to constrain the denser fluid during the movement along the slope) might be necessary to recreate the impulse wave formation and run-up at the head of Lituya Bay.**

4.2 Wave formation and run-up

A topographic and bathymetric surface of the impact area is set up and the shape of the denser fluid is readapted to the detachment area (Fig. 5, 7a). What changes in here with respect to the model concept analysis is: a) the slope angle is not constant, but ranging from 45° at higher elevation to 35° at the shoreline, b) the volume of the seawater involved in the numerical model since the deltas where not considered in the simplified simulations (about 1.73x10^{6} m^{3} of seawater respect 3.34x10^{6} m^{3} in the model concept analysis). This can have a significant influence regarding the water volume involved in the wave formation and run-up.

The main task of this part of the work is to investigate the wave features**characteristics** after the slide impact **of the denser fluid**, to simulate the maximum run-up but also to simulate the overtopping process and the flow path along the slope on the other side in respect to the Gilbert Inlet and recreate the related trimline.

The detachment area, where the rockslide failed, is confined on the left side from the topographic surface, while on the right side two scar channels are presented (Fig. 2a, 7a). These are related to other smaller slides**rockslides** that occurred during the earthquake but were not involved in the impulse wave formation (Miller, 1960). For this reason, a constraining wall (invisible in the images) is set only on the right side with respect to the rockslide described by Miller (1960). A simulation without the wall is also set up to observe the eventual rockslide**fluid** collapse and impact process.

The results obtained (Fig. 8) vary according to the adopted uniform grid resolution (20-10-5 m) (Fig. 5Even more realistic results and the observed maximum run-up in the impact area can be achieved using a uniform grid resolution of 5 m. This model, adopting the second order approach or the density evaluation, takes 1 day and 3 hours to run.

Following, a description of the wave formation and run-up resulting from the simulation with 5 m grid resolution and the adopted second order approach **for the density evaluation** is provided**. This model takes 30 hours to run**.

- *0-15 s*: The rockslide**denser fluid** reaches the sea after 12**10** seconds with a maximum velocity of 94**93** ms^{-1} and a mean**maximum** thickness of 69**79** m (P1 - x_0=45 m, Fig. 7c, **8a**). The depth averaged velocity varies from 40 ms^{-1}, in the upper part, to 90 ms^{-1} in the lower part of the slide**fluid** during the collapse**movement** (Fig. 7).
- *15-25**30** s*: After 12**24** seconds from the impact**denser fluid release** the maximum estimated wave height**amplitude** results 211**to 208** m a.s.l. with a **flow** velocity of 78 ms^{-1} (P2 - x_0=688 m, Fig. 7b). Little further (x_0=885 m) the wave maintains its height about 208 m a.s.l. to start its breaking process. A part of the wave flows also on the glacier.
- *25-35 s*: After 16 seconds from the impact a frontal flow starts to run **The wave front runs** up the delta and the following slope (Fig. 7c).9c).
- ***30-35 s:*** The whole wave crashes on the opposite headland after 22**30 seconds from the denser fluid release (20** seconds after the impact), with a variable height**water surface elevation** of 130**129**-147 m **a.s.l** and a **flow** velocity between 60-80**50-70** ms^{-1} (P3 -x_0=1342, Fig. 7c). The wave breaking stage is not complete: it partially breaks when it flows on the delta.
- *35-50 s*: The wave runs up the headland and the scars located upon the delta. The maximum observed run-up (524 m a.s.l.) is reached after 34**46** seconds from**(36 seconds after** the **denser fluid** impact, Fig. 9) with a flow height**depth** of 114**-10** m and a **flow** velocity of 4**12** ms^{-1}, having a moment of steady state, and reprising its flow with a velocity of 6 ms^{-1}. A great part**. Part** of the wave body overtops the hillcrest, but a backflow is also observed.
- *50-70 s*: The wave overtops the crest of the hill and flows on a diagonal direction compared to the slope, with a depth average velocity of 60-80**50-70** ms^{-1}. The wave reaches the seaside 8 seconds after the maximum run-up (54 seconds from the impact).**denser fluid release, Fig. 9).** The flow height**depth** is about 25**15** m with a **flow** velocity of 70 ms^{-1}. The resulting trimline is very close to the observed one (yellow dashed line Fig. 10, light blue in Fig. 12)

It is noticed that the left side the rockslide material, during the collapse process,**part of the denser fluid** is well constrained by the actual topography (Fig. 7b, c) **during the collapse process.** Avoiding the wall on the right side, the material**mass** largely spreads and collapses on the glacier, losing a great amount of volume involved in the impact process and decreasing the wave formation. The presence of the wall constrains the slide materialdenser fluid on this side and allows it to collapse in the water body. In addition, the Gilbert Glacier acts also like a constraining wall and the delta in front of the glacier as a ramp. The rockslide hitting on them features a higher velocity and wave velocity as well (Fig 8c, 9a, b).

The maximum wave heightamplitude of 208 m is located exactly upon the terminal front of the delta on the bay floor (where the history probe P2 is located, graph in Fig. 8b). In here, the wave celerity is estimated with 55 ms^{-1} (from the equation 2.2 provided by Heller et al., 2009). The wave starts to break because of its interaction with the decreasing bay floor depth. Fritz at al. (2001) observed the maximum wave height (> 200 m) at x_0=600, while at x_0=885 they reconstructed a wave height of 152 m.

The presence of the scars area on the right side of the maximum run-up has a key role in the run-up process, since it allows the wave to run-up along a channel (Fig. 9to overtop the hillcrest (exactly where the maximum run-up is recorded) and reach the elevation of 524 m a.s.l. This observation supports the topography description provided by Miller (1960). Despite the reproduction of the expected overtopping over the hill and the flow process on the other side of the slope, the resulting trimline appears underestimated compared to the observed one (light blue in Fig. 12b).

Additionally, if 524 m a.s.l. is the maximum run-up elevation observed from the trimline, this is not clear in the scars area on the right side since there are no evidences of a forest trimline. With regard to the simulation results, it appears that the maximum run-up has reached an elevation up to 600 m a.s.l. in this part of the slope.

4.3 Impulse wave propagation

The aim of these simulations is to reproduce the wave propagation along the bay, to understand how the waves interact and inundate the inland and to recreate the actual trimline. For the wave propagation, only the second order approach for the density evaluation has been used. Observation gauges for water level measurement allow more insights in the wave featurescharacteristics during the propagation and to observe the wave attenuation along the bay to the seaside (Fig. 5).

The results obtained from the simulations vary depending on the resolution of the computational grid. A description of the wave propagation and inundation resulting from the simulation with 15x15x10 m grid resolution and the adopted second order approach is provided. (details are referred to the primary wave front). The model takes 165 hours to run completely.

- *0-5060 s*: Over the impact area, the wave starts to propagate withresulting in a heightwater surface elevation of 3440 m a.s.l. and a flow velocity of 119 ms^{-1} at P4 (x_0=600, Fig. 10a).
- *50-10060-120 s*: The wave impacts on the opposite side of the bay and propagates in open sea withwater; at P5 (x_0=3100, Fig. 10b) a heightwater surface elevation of 3839 m a.s.l. and a flow velocity of 2719 ms^{-1} (P5 - x_0=3100, Fig. 11b),are recorded, due to the amount of water flowing down from the slope with high velocity. An impact on the southern side of the bay in front of the Gilbert Inlet is observed, where a secondary wave front is generated due to reflection. The primary wave front reaches the Mudslide Creek delta and floods the inland with a depth-averaged velocity of 25-3520-30 ms^{-1}. The second highest run-up results in 220overestimated with 233 m a.s.l. about 8094 seconds after the impactrelease of the rockslidedenser fluid (the observed one is 208 m a.s.l.).
- *100-180120-200 s*: The wave splits into two fronts approaching and impacting Cenotaph Island (25water surface elevation of 22 m a.s.l. and 128 ms^{-1} of flow velocity, recorded at P6, x_0=5600, Fig. 10c). On the

southern side, where the bay floor has its deepest depth (-220 m a.s.l.), the wave **slightly** slows down due to the constriction between the island and the bay shoreline, increasing its height resulting in 29 m **attenuation process,** with a **water surface elevation of 19 m a.s.l. and a flow** velocity of 75 ms^{-1} at P7S (x_0=6600). The steep slopes on the southern side of the bay are completely flooded

- *180-280 s*: **by the wave (Fig. 10d).** On the contrary, on the northern side of the island, where the bay floor gets more shallow (**depth** 20-40 m depth) and narrow, the wave height**water surface elevation** results in 2615 m **a.s.l.** with a velocity of 147 ms^{-1} at P7N (x_0=6600, Fig. 12d). This is probably due to a breaking process.
- ***200-280 s*:** Due to diffraction, the waves turn around the island and flood the western side of Cenotaph Island. The two fronts converge again to one wave **(front from the southern channel comes first, as observed at** P8 (x_0=8100, Fig. 10d,e) **resulting in** a flow velocity of 54 ms^{-1} and a wave height**water surface elevation** of 1210 m **a.s.l**. The flatter northern side of the bay is flooded **(Fig. 10e).**
- ***280-340 s*:** The wave reaches the maximum distance of 1400 m flooding the area in front of Fish Lake with a depth-averaged velocity of 10-25 ms^{-1} and according wave heights of 10-5 m.**an according water surface of 15-5 m from the ground (Fig. 10f). The wave approaches to the mouth of the bay, resulting in a water surface elevation of 13 m a.s.l and a flow velocity of 5 ms^{-1} at P9 (x_0=10600, Fig. 10f). The second wave front reaches the first one, resulting in a long period wave; it takes 180 seconds to pass over the history probe P9 (from 240 seconds to the time limit of the simulation, 420 seconds).**
- *280-380 s*: The wave approaches to the ending and narrow part of the bay, resulting in a front of 16 m and proceeding with a velocity of 5 ms^{-1} (P9 - x_0=10600, Fig. 11f). The wave appears to be a long period wave; it takes 180 seconds to pass over the spot of P9 (from 240 seconds to the time limit of the simulation, 420 seconds).
- *380**340**-420 s*: After 380**340** seconds **from the release of the denser fluid** the wave reaches the sea side**seaside**, flooding completely La Chaussee Spit and the nearby areas with a depth-averaged velocity of 10-20 ms^{-1}.

The main wave generated by the rockslide's impact into the water body seems to be the main**is mainly** responsible for the forest destruction, but secondary reflected waves along the bay also contribute to the observed trimline. A clear example is the wave reflected from the Mudslide Creek impacting the opposite northern slope of the bay at 140 seconds (Fig. 10c). Other secondary wave fronts spread from the bay head due to several reflections of the backflow in front of the Gilbert Inlet.

The resulting trimline from the simulation with a grid resolution of 15x15x10 m is the closest to the observed trimline (Fig. 12). Some discrepancies are observed. Some areas are **In Figure 11a the wave propagation in time for the primary wave front is illustrated. The reported values represent a mean value of propagation speed for each space interval, starting from the records provided by the gauges located along the bay, considering the wave front position at the time of its passage upon every singular gauge (Fig. 11b) and adopting flow path lines for distance estimation. The wave attenuation process, both in terms of wave amplitude (from 40 to 18 m) and mean propagation velocity decreases (from 40 ms^{-1} to 17 ms^{-1}), proceds from the head of the bay until the seaside. Higher values of the mean velocity are found between P4 and P5 (due to the water flowing down from the slope and impacting the sea with high velocity, thus accelerating the wave) and** between P7S and P8 (due to the deepest bay floor, inducing a local increase of the wave propagation velocity). Dashed lines represent the secondary wave in time. Its role becomes relevant after the gauge P6: the second front approaches the first one evolving in a whole wave body between P9 and La Chausse Spit (C.S. in the graph), inducing an increase of the wave amplitude (from 13 to 18 m) before the breaking process.

Independently from the grid resolution, general discrepancies in the trimline definition are observed (Fig. 12a,b). Some areas result underestimated, as for example the slopes on the othersouthern side of the bay in front of the Gilbert Inlet, southern than the head, the western part of Crillon Inlet, and the Mudslide Creek and eastern than Fish lake.location. Others are overestimated, as some areas along the southern side of the bay at the Cascade Glacier location, the second highest run-up overafter the Mudslide Creek and western than Fish Lake. Using a grid resolution of 15x15x10 m the eroded channel in southern of Cenotaph Island has not been reproduced; while this.

The adoption of different values of relative roughness for the topographic surface (0-1-2 m, Fig. 12c) results in an evident change for the inundation process. As shown in Figure 12c, important differences in the flooded area are evident on flatter locations, mainly presented in the western region of the bay. Additionally, adopting a roughness of 2 m, the second maximum run-up at the Mudslide Creek results in 210 m a.s.l. Therefore, the trimline obtained from the simulation with 2 m of relative roughness, for a grid resolution of 15x15x10, is very close to the observed one, even if some small under and overestimation are still present. However, it is noticed that also the simulation with a uniform grid resolution of 20 m can reproduce the tsunami trimline well.

The fluids mixture process and the submerged propagation of the rockslide materialdenser fluid along the bay ground can be notedfloor takes place using the second order approach for the density evaluation (Fig. 13).. At the end of the simulation the materialdenser fluid reaches a distance of almost 5up to 4 km from the impact point, still propagating with a low velocity of 85 ms^{-1} and a thickness about 35 m. The bulk slide density variesof the denser fluid decreases during the propagation from 1620 kgm^{-3} to approximately 12601080 kgm^{-3}. The described process is not perfectly realistic since all the material that contributes to infill the bay (the material generated from the deltas displacement, the sediment released by the glacier and the eroded soil from the inland) is not simulated due to a lack in information about the volumes involved and due to software limits to reproduce multiphase and thin layers. Anyway, this option represents a suitable approach to qualitatively reproduce the submerged propagation of materials into a water bodies, like turbidity currents, which is close to the seawater density.

5 Discussion

To accurately simulate landslide-generated impulse wave dynamics in lakes (or fjords) and inundation processes, a high-quality and detailed reconstruction of the bay configuration pre-event is required, especially in areas where the wave featurescharacteristics (as height and velocity) change rapidly and drastically (as in the impact area). No high -resolution data pre and post 1958-event, as bathymetry and topography, are available for the Lituya Bay. The use of the most recent DTM together with data and information provided by several sources for the case study area and the bay bathymetry before and after the event allows a reliable but not fully exact reconstruction of the bay configuration previously to the event. This has a high influence on the model performance and its outputs.

Different uniformThe use of virtual walls and their effects was first investigated in the model concept analyses before being considered in the simulations with the topographic surface (section 4.1 and 4.2). The absence of the walls allows the fluid volume to expand during the movement process, while the presence of the walls constricts the fluid until the impact into the sea. This mostly influences the wave characteristics close to the impact location during the propagation phase and the further run-up on the opposite slope.

In the simulations with the topographic surface, the topography performs as a normal constriction for the dense fluid at the SE boundary of the scar area (Fig. 7). While on the NW border the presence of the wall has been adopted as a simple solution to compensate the lack of topographic elements due to the presence of scars related to secondary rockslides not involved in the wave generation (Fig. 2a). Since it is understood that almost all the main rockslide volume impacts the water body and generates the impulse wave, the presence of the virtual wall avoids the lack of a part of the moving denser fluid volume to impact the water body. In the contrary case, it would disperse and impact on the glacier, resulting in a decrease of wave amplitude and run-up.

Uniform and non-uniform computational meshes with different grid resolutions have been used to simulate the wave formation and propagation. For the impact area uniform mesh blocks are set, with resolutions of 20-10-5 m. For the whole bay, uniform and non-uniform resolutions as 20x20x20 m, 20x20x10 m, 15x15x10 m are used. As expected, the outputs vary according to the resolution of the simulation, where the higher the resolution, the better the. More accuracy of the results. Thisfor finer meshes is due to more accuracy in the computation process and the generated computation surface (e.g. roughness), resulting in more preciseaccurate representation of the natural bathymetry and detailed than the ones generated by larger resolutions. topography.

In the impact area, it appears that the rockslidedenser fluid and wave featuresflow characteristics, using a uniform grid resolution of 20 m, result in lower values respect to the ones obtained with a grid resolution of 5 m, except for the waveflow velocity at x_0=1342 m and for the rockslide thickness of the denser fluid (graphs in Fig. 8a).

Concerning the wave propagation (water surface elevation and its features trend (maximum wave height and waveflow velocity, graphs in Fig. 10), it is noticed, that a grid resolution of 20x20x10 m roughly approximates the results using a grid resolution of 15x15x10 m. Adopting a resolution of 20x20x20 m results mostly in an over- or underestimation of the wave features trendcharacteristics, where a delay, compared to the other trends, of a few to 12 seconds can be observed.

Concerning grids and the limits with regard to the computation times, the resolution of 15x15x10 m leads to the maximum manageable number of cells for this model (880875 cells involved in the computation). A resolution of 10x10x10 has been tested, but the calculation stops after 20 % of run, probably due to excessive requested power and memory.

The influence of different grid resolutions on the outputs can be clearly observed in the estimated run-up (In order to verify improvements of the outputs accuracy for finer used resolutions, a conformation of difference reduction in flow characteristics values, between each refinement, is provided. The percentage difference and root mean square error (RMSE), starting for the series of data recorded from the gauges, are thus estimated. The finest used mesh (15x15x10 m) is taken as a standard. Concerning the water surface elevation, the estimate shows an improvement of the accuracy of the resulting data with a percentage difference of -39 ± 119 (RMSE of 4.83 m) and -16 ± 68 (RMSE of 2.25 m) from the uniform resolutions of 20 m and non-uniform one of 20x20x10 m. An improvement of the accuracy of the flow velocity with a percentage difference of -21 ± 62 (RMSE of 2.02 ms^{-1}) and -16 ± 45 (RMSE of 1.07 ms^{-1}) from the resolutions of 20 m and 20x20x10 m is also noticed. This comparison of the computational results covers water surface

elevations and velocities not only for the local maxima but during the entire simulation periods. This means that already small temporal delays in wave propagation lead to distinctive statistical parameters when comparing two simulations with nearly identical maxima of amplitude and flow velocities with each other.

The influence of different grid resolutions on the outputs can be clearly observed in the estimated run-up (cross sections in Fig. 13). Adopting the second order approach for the density evaluation, the maximum run-up , in the impact area results to 390 m a.s.l., 450 m a.s.l. and 524 a.s.l. m for a uniform grid resolution respectively of 20-10-5 m (Fig. 13a). The second highest run-up at Mudslide Creek results to 209 m a.s.l., 220 m a.s.l. and 233 m a.s.l. for a grid resolution of 20x20x20 m, 20x20x10 m, 15x15x10 m respectively (Fig. 13b). **The present divergence with mesh refinement, for the run-up values in the two different locations, is explained considering the 3D effect of the topography and the direction of the wave approaching the inland and runs upon the topographic surface (from the front in case of section A-A´ and from the side in case of section B-B´).**

Discrepancies in resulting trimline with respect to the observed one (Fig. 12) can be related to different sources: a) to computation errors propagation, b) to the impossibility to sufficiently reduce the grid resolution given the required computational power and memory, c) errors in the reconstruction of the bathymetry, topography and shoreline in some areas of the bay, thus a not adequate seawater volume to generate the wave, and d) the adoption of a smooth surface (zero relative roughness) for the topography surface. e) only the rockslide has been considered as impulse wave trigger

Some instabilities occurred during the calculation for the finer meshes. These are noticed to be mostly caused by isolated fluid drops as result of free surface breakup (persistent fraction packing locations due to high splashing or foaming; Vanneste, 2012). To avoid instabilities, the CFPK (fraction packing coefficient) has been reduced by a factor of 10 in the advance numerics option in Flow-3D.

The estimated trimline, for the coarsest resolution used (uniform - 20 m), results in an evident underestimation at Gilbert Inlet but, on the contrary, mostly an overestimation**appears to be quite close to the observed one** along the whole bay. An intermediate grid resolution (uniform - 10 m in the impact area and non-uniform - 20x20x10 m for the whole bay) gives still an underestimated trimline at Gilbert Inlet, and results in a slight overestimation along the entire bay. The finest grid resolution used (uniform – 5 m in the impact area and non-uniform – 15x15x10 m for the whole bay) results in a more accurate trimline, closer to the observed one, even though some under- and overestimations are still obvious. The adoption of a relative roughness **than 1 m avoids some of these overestimations, bringing the resulting trimline closer to the observed one. Additionally, it is observed that a value of roughness higher than 0 m avoids the splashing of water on the topographic surface, allowing an easier definition of the inundated area and a shorter simulation duration**.

Concerning the use of different order approaches for the density evaluation, some considerations are proposed. In the simulations with the actual topography and bathymetry shape, using a uniform grid resolution of 20 m, the use of the first order approach underestimates much more the observed maximum run-up of 524 m a.s.l., resulting in 418 m a.s.l. compared to the one obtained with the second order approach (463 m a.s.l.) (Fig. 14a). This difference is reduced when an uniform grid resolution of 10 m is used, resulting in 500 m a.s.l. and 510 m a.s.l. respectively for the first and second order approach. Adopting a uniform grid resolution of 5 m the maximum run-up of 524 m a.s.l. is obtained independent of the order approach for the density evaluation. This highlights the key role of the resolution of the computational grid and its influence on the outputs accuracy and, in part, how the characteristics of the rockslide during the impact process in the water body influences the wave features and run-up heights, regardless of the used approach.

On the other side, it**Concerning grids and the limits with regard to the computation times, the resolution of 15x15x10 m leads to the maximum manageable number of cells for this model (total cells: 50,458,234; active fluid cells: 7,254,191; solid sub-domain cell: 835,184). A resolution of 10x10x10 has also been tested (active fluid cells: 16,176,884). Despite the use of a more powerful machine (and a parallel license tokens using 32 cores), the simulation could not be completed within a couple of weeks. This can be due of high instability in the model, possibly related to splashing (a reduced value of CFPK did not avoid instabilities in this model).**

It is noticed that the mixing process between the two fluids strongly depends on the order approach for the density evaluation. As showed in Fig. 14a, b, c the first order allows the fluids to mix fast immediately after the impact, during the air cavity collapse and the run-up. Whereas with the second order approach (Fig. 14d, e, f), separation of the fluids is much more remarkable. The use of specific order affects the slide material behavior during its run-out process, where the first order approach leads to a larger dispersion of the denser fluid inside the seawater.

Simulations were also performed with different values of the relative roughness, respectively 0-1-3 m (representative of the vegetation height in the bay). However, no differences in the inundation process and trimline definition are observed. It is supposed that with the use of a larger cell size and the related generated computational surface, together with the presence of mostly steep slopes and the great energy involved during the wave propagation, different values of relative roughness are not relevant. This issue will be more investigated in following works.

The described mixing process in section 4.3 is not representative for the Lituya Bay rockslide underwater run-out, since the denser fluid model is adopted at the Gilbert Inlet to recreate the sliding body. Regarding the material deposited in the bay after the tsunami event, and considering the available information provided by literature (section 3.1), it is plausible to consider that the disintegrated rockslide mass did not totally infill the bay floor. The contribution of the material generated from the deltas displacement, the sediment released by the glacier and the eroded soil from the inland has to be as well taken into account.

6 Conclusion

In this study, the Lituya Bay 1958 tsunami event was reproduced. With respect to previous works, we did a step**provide an improvement** over the studies that limit to reproduce**in reproducing** the physical scale test of Fritz et al. (2001), recreating the bay configuration pre-event and adopting a specified dataset provided by literature. From the numerical modelling perspective, while most of the previous simulations were setup in 2D, we adopted a 3D-numerical modelling approach implemented in Flow-3D to recreate the wave dynamics in the whole bay. We tried to give a better comprehension of the**In this way, we expanded existing knowledge on this complex physical** phenomenon itself and provided more insights about**regarding** the wave formation, propagation and the 3D effects on the wave features**characteristics** due to the interaction with the recreated bay surface.

The simulations results show the complexity of the physical phenomena itself and prove**Our results attest** that a good model can represent what actually happened during the entire event and give a better understanding of the Lituya Bay tsunami event on 9 July 1958. A detailed knowledge of the case study helps us to evaluate the reliability of the outputs. The impact area and the whole inundated bay have to be analysed separately to get more details into the entire process.

The reconstruction (or definition) of a realistic, reliable and detailed bathymetry and topography is fundamental**recommended** for an impulse wave simulation since the surface generated by the computation grid influences the definition of the inundated area during wave propagation and inundation. Having reliable bathymetry data, realistic depth and shape information of the bay floor before the event enables the simulation of a reliable interaction between the impulse wave and the bay floor, e.g. to observe the wave behavior during its propagation (breaking process or maintaining its shape and characteristics).

A detailed topography allows simulating a trimline as similar as possible to the observed one. This is depending on the surface generated by the computation grid and its spatial resolution. A high grid resolution can highlight topography details that can be fundamental to estimate the flooded area. The definition of the pre-event shoreline is relevant, mostly where it has been extremely modified by the tsunami event. This happens principally in the impact area, where the rockslide entered into the water body and the tsunami featured highest intensities (in terms of velocity and water height). **In general, this highlights the need for adequate pre-event information of the terrain, especially in regions with lower water depths and impact with the surrounding ground.**

The following main conclusions are reported:

- The simplified analyses are in good agreement with previous studies (e.g.**model concept analysis reliably reflects results from experiments and numerical simulations proposed by** Fritz et al., **.** (2001,**) and** Basu et al., 2009).**. (2010), despite an overestimation of the run-up values.** It is observed that a "dense fluid" is a suitable, simple concept to recreate the impact of a sliding mass in a water body, in this case with an impact velocity between 93-104**about of 92-114** ms^{-1}. **(for a slope inclination of 35 degrees, Fig. 6c).** For this concept, the use**consideration** of the bulk slide volume and the bulk slide density is fundamental for an adequate for the reproduction of the rockslide. Besides, a method to simulate the slide material with the real dimensions and properties has still to be found with Flow-3D.**impact intensity.** The presence of the Gilbert Glacier and **virtual** walls to constrain the slide material during the collapse process has a crucial influence on wave formation and run-up.
- It is demonstrated that the rockslide represents the main trigger for the impulse wave generation in Lituya Bay (as proposed by Fritz et al., 2009), **and for the forest destruction under the trimline.** The slide collapse**simulated fluid impacts** into the water body reproduces the wave dynamics and run-up at Gilbert Inlet. It also represents the primary trigger for the wave propagation along the whole bay, the related**including water surface elevation,** wave features and dynamics as wave heights, wave velocity**propagation speed**, inundation effects and trimline definition. On the other side, it can be confirmed that the rockslide material alone does not explain the total infill of the bay bed after the 1958 tsunami event.
- The resulting maximum wave height**amplitude** of 211**208** m a.s.l. and the maximum run-up of 524 m a.s.l. are obtained using a uniform mesh size of 5 m. Even though the simulation shows the wave overtopping the hill **facing the slide source**, then flowing diagonally **downslope,** the slopes, recreating in an accurate way most of**simulations still significantly underestimate** the observed trimline.
- A mesh size of 15x15x10 m is required for a reliable simulation of the wave **dynamics** propagation along the whole bay. The estimated trimline **fits best to the observed one when a relative roughness of 2 m** is the result**set for the vegetated part of the topographic surface. The inundation is caused** not only

by the primary wave but also by several secondary reflected waves. It is observed that the wave reacts to the bathymetry and topography shape, varying its features during the propagation and evolving from a high-velocity, steep-front wave at the head of the bay, to a slow-velocity, long-period wave when approaching the seaside.

- The use of different order approaches for the density evaluation has been tested, resulting in a large variability of**different behavior for** the results when a low grid resolution is adopted (e.g. 20 m), not influent in the wave features or run-up height when a grid resolution of 5 m is applied. A mixing process between the two fluids, **occurring faster for the first order approach. No important influences on the wave amplitudes and run-up heights are** observed.
- The **relative difference and the RMSE for the water surface elevation and flow velocity values highlight the improvement in accuracy when adopting a finer** mesh. **In general, this work supports** the necessity to use a grid resolution as high as possible for a reliable model of a landslide-generated impulse wave and to obtain accurate outputs. **and insights in the wave dynamics.**
- The results confirm that the bay configuration before the tsunami event has been reconstructed well and support the descriptions provided by Miller (1960). The possibility to have direct available data concerning the bathymetry and topography before and after a tsunami event makes the interpretation and reconstruction of the case study easier and more precise. The lack of data and limited information concerning the Lituya Bay 1958 tsunami event obligates experts to give their own subjective interpretation; the possibility of some errors and inaccuracies is higher.

Following these remarks and what has been discussed in section 5, some considerations in terms of computational effort vs. trimline reliability are proposed. Utilizing the same computational resource (see section 3.2.1), the wave propagation model with an uniform grid resolution of 20 m already gives a trimline quite close to the observed one with a calculation time of 3 hours. Adopting a finer resolution of 15x15x10 m, even if the trimline results more accurate, overestimations are still noticed. The calculation takes time of almost 7 days to run. This high computational time can be still considered as an affordable one for a numerical model simulations. Despite this, in an application for a hazard analysis, a model with a coarser resolution can represent a fast and sufficient solution for a rough assessment of a landslide-generated impulse wave event, where it is possible to obtain already a good approximation of the inundated area. Anyway, in order to get more details and insights for the wave dynamics, models with a finer mesh are recommended, where different scenarios adopting different values for the topographic surface roughness have to be tested.

Concluding, the Flow-3D software represents a suitable tool for landslide-generated impulse wave simulations. **The software can provide a good approximation for the impact process with the limitations of the chosen modeling concept regarding the representation of the physics of the impact process.** Some discrepancies in the inundation dynamics and the trimline estimation still occur in the model. This can be explained by the software limits, computational errors, and imprecision in the bay reconstruction due of lack of information. **It has to be said that observation data are also not always and everywhere perfectly represented.**

Concerning future works, research and tests on other available tools in Flow-3D (like the drift-flux model or the general moving object model), useful to reproduce a sliding mass impacting a water body, will be proposed.

With regard to the last research questions concerning the application of this 3D-numerical approach and its capabilities (section 1), this work shows the value and applicability of models like this not only for back-calculating and recreating past events, but for risk assessment in areas potentially endangered by large impacts in fjords and lakes. The shape of the Lituya Bay, as a narrow and long fjord, and the gravitational process that generated the impulse wave (a rockslide evolved in a rock avalanche) represent a situation that can be easily found also in other mountain regions as the Alps.

Data availability

Simulation videos and additional data (reconstructed bathymetry and topography) that support the findings of this study are available on the following link:
https://www.uibk.ac.at/alpinerraum/dps/dp-mountainhazards/scienceflash/franco.html.en.
The original DTM-data is available from the DGGS Elevation Portal, the bathymetry data from the National Ocean Service: Hydrographic Surveys with Digital Sounding (Survey IDs: H08492, 1959; H04608, 1926).

Authors contributions

AF designed the case study and the main research goals, with support from BG concerning the modelling in Flow 3D. AF prepared the manuscript with contributions of JM, BSM, MS and BG. All authors discussed, reviewed and edited the different versions of the manuscript.

Competing interests

The authors declare that they have no conflict of interest.

Acknowledgements

This research is funded by the University of Innsbruck in support of the doctoral program "Natural Hazards in Mountain Regions". It is related to the research project "Wave formation, propagation and run-up in natural mountain lakes from a cascade hazard perspective – analysis and modeling of triggering processes, lake´s morpho-dynamics and potential downstream hazard effects". A great thank is also owned to the (anonymous) reviewers whose comments and remarks greatly improved the models set-up, quality of the achieved results, clarity and finally the quality of this manuscript.

References

Basu, D., Das, K., Green, S., Janetzke, R., and Stamatakos, J.: Numerical simulation of surface waves generated by subaerial landslide at Lituya Bay Alaska, Offshore Mech Arct Eng, 132, 11, https://doi.org/10.1115/1.4001442, 2010.

Braathen, A., Blikra, L.H., Berg, S.S., Karlsen, F.: Rock-slope failures in Norway; type, geometry, deformation mechanisms and stability, NGT, 84, 67-88, 2004.

Bridge, T.: When mountains fall into the sea. www.hakaimagazine.com, 2018. Date of access 09.2018

Chuanqi, S., Yi, A., Qiang, W., Qingquan, L., Zhixian, C.: Numerical simulation of landslide-generated waves using a soil-water coupling smoothed particle hydrodynamics model, Adv Water Resour, 92 (2016), 130-141, doi.org/10.1016/j.advwatres.2016.04.002, 2016.

Das, K., Janetzke, R., Basu, D., Green, S., Stamatakos, J.: Numerical Simulations of Tsunami Wave Generation by Submarine and Aerial Landslides Using RANS and SPH Models, 28th International Conference on Ocean, Offshore and Arctic Engineering, Honolulu, USA, 5 (2009), 581-594, https://doi:10.1115/OMAE2009-79596, 2009.

DGGS Elevation Portal, Division of geological and geophysical survey: https://elevation.alaska.gov. Date of access 09.2018

Elliott, J., Freymueller, J.T. and Larsen C.F.: Active tectonics of the St. Elias orogen, Alaska, observed with GPS measurements, Earth Sci Res J, 5625-5642, https://doi.org/10.1002/jgrb.50341, 2013.

Flow Science Inc.: Flow-3D®, Version 12.0, User's Manual [Computer software], Santa Fe, https://www.flow3d.com, 2018.

Fritz, H.M., Hager, W.H. and Minor, H.E.: Lituya Bay case: Rockslide impact and wave run-up, Sci Tsunami Hazards, 19(1), 3-22, 2001.

Fritz, H. M., Mohammed, F., and Yoo, J.: Lituya Bay landslide impact generated mega-tsunami 50th anniversary, Pure Appl Geophys, 166, 153-175, https://doi:10.1007/s00024-008-0435-4, 2009.

Furseth, A.: Dommedagsfjellet - Tafjord 1934, Gyldendal Norsk Forlag A/S, 1958.

Gauthier, D., Anderson, S.A., Fritz H.M., Giachetti, T.: Karrat Fjord (Greenland) Tsunamigenic landslide of 17 June 2017: initial 3D observations, Landslides, 15, 327-332, https://doi.org/10.1007/s10346-017-0926-4, 2018.

Gonzalez-Vida, J.M., Macías, J., Jesús, M.C., Sánchez-Linares, C., de la Asunción, M., Ortega-Acosta, S., Arcas D.: The Lituya Bay landslide-generated mega-tsunami - numerical simulation and sensitivity analysis, Nat Hazard Earth Sys, 19, 369-388, https://doi.org/10.5194/nhess-19-369-2019, 2019.

Haeussler, P. J., Gulick, S.P.S., McCall, N., Walton, M., Reece, R., Larsen, C., Shugar, D.H., Geertsema, M., Venditti, J.G. and Labay, K.: Submarine deposition of a subaerial landslide in Taan Fjord, Alaska, J Geophys Res-Earth, 123, 2443-2463, https://doi.org/10.1029/2018JF004608, 2018.

Hall, J.V, Jr. and Watts, G.M.: Laboratory investigation of the vertical rise of solitary waves on impermeable slopes, U.S. Army Corps of Engineers, Beach Erosion Board, 173-189, 1953.

Harlow, F.H. and Welch, J.E.: Numerical Calculation of Time-Dependent Viscous Incompressible Flow, Physics of Fluids, Volume 8, 2182-2189, https://doi.org/10.1063/1.1761178, 1965.

Heller, V., **Hager,W. H., and Minor, H.-E.: Landslide generated impulse waves in reservoirs – Basics and computation, VAW Communications, 211, Laboratory of Hydraulics, Hydrology and Glaciology (VAW), ETH Zurich, 2009.**

Heller, V., Hager, W.H.: Impulse product parameter in landslide generated impulse waves, J. Waterw. Port Coast. Ocean Eng.,, 136, 145––155, https://doi: 10.1061/(ASCE)WW.1943-5460.0000037, 2010.

Hinze, J. O.: Turbulence, McGraw-Hill, New York, 1975.

Hirt, C.W. and Nichols, B.D.: Volume of Fluid (VOF) Method for the Dynamics of Free Boundaries, J Comput Phys, 39, 201-225, https://doi.org/10.1016/0021-9991(81)90145-5, 1981.

Hirt, C.W. and Sicilian, J.M.: A Porosity Technique for the Definition of Obstacles in Rectangular Cell Meshes, Proceedings of the Fourth International Conference on Ship Hydrodynamics, National Academy of Sciences, Washington, DC, 1-19, 1985.

Holmsen, G.: De siste bergskred i Tafjord og Loen, Norge, Svensk geografisk Arbok 1936, Lunds Universitet, Geografiska Institutionen Meddelande, 124, 171-190, 1936.

Huber, A., and Hager, W.H.: Forecasting impulse waves in reservoirs, Dix-neuvie`me Congre`s des Grands Barrages C31, Florence, Italy, Commission International des Grands Barrages, Paris, 993-1005, 1997.

Kamphuis, J.W. and Bowering, R.J.: Impulse waves generated by landslides, Coast Eng Proc, 35, 575-588, https://doi.org/10.9753/icce.v12.35, 1970.

Koehler, R.D.: Quaternary faults and folds (QFF), Alaska Division of Geological & Geophysical Surveys Digital Data Series, 3 http://doi.org/10.14509/24956, 2013.

Körner H. J.: Reichweite und Geschwindigkeit von Bergstürzen und Fliessschneelawinen, Rock Mechanics, 8-4, 225-256, 1976.

Mader, C.L.: Modelling the 1958 Lituya Bay mega-tsunami, Sci Tsunami Hazards, 17, 57-67, 1999.

Mader C.L and Gittings M.L.: Modelling the 1958 Lituya Bay mega-tsunami II, Sci Tsunami Hazards, 20, 241-250, 2002.

Miller, D.: Giant Waves in Lituya Bay, Alaska: A Timely Account of the Nature and Possible Causes of Certain Giant Waves, with Eyewitness Reports of Their Destructive Capacity, Professional paper, US Government Printing Office, 49-85, 1960.

Noda, E.: Water waves generated by landslides, Journal of the Waterways, Harbors and Coastal Engineering Division, 1970, Vol. 96, Issue 4, 835-855, 1970.

Pastor M, Herreros I, Fernndez Merodo J.A, Mira P, Haddad B, Quecedo M, González, E., Alvarez-Cedrón, C., Drempetic, V.: Modelling of fast catastrophic landslides and impulse waves induced by them in fjords, lakes and reservoirs, Engineering Geology, 109, Issues 1-2, 124–134, https://doi.org/10.1016/j.enggeo.2008.10.006, 2008.

Paronuzzi, P., Bolla, A.: The prehistoric Vajont rockslide: an update geological model, Geomorphology, 169-170, 165-191, https://doi: 10.1016/j.geomorph.2012.04.021, 2012.

Pararas-Carayannis, G.: Analysis of mechanism of tsunami generation in Lituya Bay, Sci Tsunami Hazards, 17, 193-206, 1999.

Quecedo, M., Pastor, M., and Herreros, M.: Numerical modelling of impulse wave generated by fast landslides, Int J Numer Meth Eng, 59, 1633-1656, https://doi.org/10.1002/nme.934, 2004.

Rady, R. M. A. E.: 2D-3D Modeling of Flow Over Sharp-Crested Weirs, Journal of Applied Sciences Research, 7, 12, 2495-2505, 2011.

Slingerland, R.L. and Voight, B.: Occurrences, properties, and predictive models of landslide-generated water waves, Developments in Geotechnical Engineering 14B, Rockslides and avalanches 2, Engineering Sites, Elsevier Scientific Publishing, Amsterdam, 317-397, 1979.

Schwaiger, H. F. and Higman, B.: Lagrangian hydrocode simulations of the 1958 Lituya Bay tsunamigenic rockslide, Geochem Geophys Geosyst, 8, Q07006, https://doi.org/10.1029/2007GC001584, 2007.

Sepúlveda, S. A., A. Serey, M. Lara, A. Pavez, and Sepúlveda, S.A., Serey, A., Lara, M., Pavez, A., Rebolledo, S.: Landslides induced by the April 2007 Aysén Fjord earthquake, Chilean Patagonia, Landslides, 7, 483-492, https://doi 10.1007/s10346-010-0203-2, 2010.

Sharpe, C.: Landslides and Related Phenomena, Columbia Univ. Press, New York, 1938.

Synolakis, C.: The runup of solitary waves, J Fluid Mech, 185, 523-545, https://doi:10.1017/S002211208700329X, 1987.

Tocher, D. and Miller D.J.: (1959) Field observations on effects of Alaska earthquake of 10 July, 1958, Science, 129, 3346, 394-395, https://doi:10.1126/science.129.3346.394, 1959.

Tognacca, C.: Beitrag zur Untersuchung der Entstehungsmechanismen von Murgangen, VAW communications, 164, Laboratory of Hydraulics, Hydrology and Glaciology, ETH Zurich, 1999.

US Coast and Geodesic Survey: Survey id: H04608: NOS Hydrographic Survey, 1926-12-31, available at: https://data.world/us-noaa-gov/f6786b28-ea06-4c9a-ac30-53cb5356650c, 1926.

US Coast and Geodesic Survey: Survey id: H08492: NOS Hydrographic Survey, Lituya Bay, Alaska, 1959- 08-27, available at: https://data.world/us-noaa-gov/ 9401821a-28f5-4846-88db-43e702a5b12b, 1959.

U.S. Coast and Geodetic Survey (1942), Chart 8505, Lituya Bay.

U.S. Coast and Geodetic Survey (1969), Chart 8505, Lituya Bay.

U.S. Coast and Geodetic Survey (1990), Chart 16762, Lituya Bay.

Vanneste, D.: Experimental and numerical study of wave-induced porous flow in rubble-mound breakwaters, PhD Thesis, Gent University, Gent, Belgium, 2012.

Varnes, D.: Landslide type and Processes, In Landslides and Engineering Practice, H R B Special Rep., Vol. 29, 22-47, National Research Council (US), 1958.

Vasquez J.A.: Modelling the generation and propagation of landslide-generated landslide, CSCE SCGC, Leadership in Sustainable Infrastructure, Annual Conference, May 31 - June 3, Vancouver, 2017.

Yakhot, V. and Smith, L.M.: The Renormalization Group, the e-Expansion and Derivation of Turbulence Models, J Sci Comput, 7, 35-61, https://doi: 10.1093/gji/ggv026, 1992.

Wang, J., Ward S.N., Xiao, L.: Numerical simulation of the December 4, 2007 landslide-generated tsunami in Chehalis Lake, Canada, Geophys J Int, 201, 372-376, https://doi: 10.1093/gji/ggv026, 2015.

Ward S.N. and Day, S.: The 1958 Lituya bay landslide and tsunami – A tsunami ball approach, J Earthq Tsunami, 4 (4), 285-319, https://doi: 10.1142/S1793431110000893, 2010.

Weiss, R. and Wuennemann, K.: Understanding tsunami by landslides as the next challenge for hazard, risk and mitigation: Insight from multi-material hydrocode modeling, American Geophysical Union, Fall Meeting 2007, abstract id. S51C-06, 2007.

Weiss, R., Fritz, H. M., and Wünnemann, K.: Hybrid modeling of the mega-tsunami runup in Lituya Bay after half a century, Geophys Res Lett, 36, L09602, https://doi.org/10.1029/2009GL037814, 2009.

Welch, J.E., Harlow, F.H., Shannon, J.P. and Daly, B.J.: The MAC Method: A Computing Technique for Solving Viscous, Incompressible, Transient Fluid Flow Problems Involving Free-surfaces, Los Alamos Scientific Laboratory report LA-3425, 1966.

Wiegel R.L.: Oceanographical Engineering, Englewood Cliffs, New Jersey: Prentice Hall, 1964.

Xenakis, A.M., Lind S.J., Stansby, P.K. and Rogers, B.D.: Landslides and tsunamis predicted by incompressible smoothed particle hydrodynamics (SPH) with application to the 1958 Lituya Bay event and idealized experiment, Proceedings of the Royal Society A, https://doi: 10.1098/rspa.2016.0674, 2017.

Table 1: Summary of the governing parameters of the Lituya Bay 1958 tsunami event and related references.

Data	Symbol	Dimension	Value	References
Water depth (impact area)	*hw*	m	*122*	Miller, 1960; Slingerland and Voight, 1979; Fritz et al., 2001
Seawater density	*ρw*	kgm^{-3}	*1035*	Basu et al., 2010
Slide height (thickness)	*sh*	m	*92*	Miller, 1960; Slingerland and Voight, 1979; Fritz et al., 2001
Bulk slide height	*Sh*	m	*134*	Fritz et al., 2001
Slide length	*ls*	m	*970*	Miller, 1960; Slingerland and Voight, 1979; Fritz et al., 2001
Slide impact velocity	*vs*	ms^{-1}	*90-110*	According to eqation 3.1 from Heller et al., 2009, with a dynamic bed friction angle δ 14 degrees; Slingerland and Voight, 1979, Fritz et al., 2001
Grain volume	*Vg*	m^3	30.6×10^6	Miller, 1960; Slingerland and Voight, 1979 ; Fritz et al., 2001
Bulk slide volume	*Vs*	m^3	51.0×10^6	Heller et al., 2010
Grain density	*ρg*	kgm^{-3}	*2700*	Miller, 1960; Slingerland and Voight, 1979; Fritz et al., 2001
Bulk slide density	*ρs*	kgm^{-3}	*1620*	Heller et al., 2010
Impact slope angle	*α*	°	*35-45*	Miller, 1960; Fritz et al., 2001
Porosity	*n*	%	*40*	Fritz et al., 2001
Maximum run-up	-	m a.s.l.	*524*	Miller, 1960; Fritz et al., 2001
Maximum wave height	-	m a.s.l.	*>200*	Fritz et al., 2001

Table 2: Summary of the simulation setup and modelling tasks.

Model	Grid resolution [m]	Domain extent [m]	Number of cells: total; active fluid [-]	Simulation time [s]	Modelling task
Concept analysis (for 45 ° slope inclination)	*10x10x10*	*3190 x 2220 x 1120*	***8,233,657; 2,282,450***	*60*	Test of the denser fluid concept and its effects on the wave formation and run-up in the simplified bucket model
Impact area	*20x20x20* *10x10x10* *5x5x5*	*1600 x 4000 x 1200*	***1,089,596; 423,833*** ***8,435,576; 3,073,436*** ***66,376,736; 23,153,232***	*70*	Recreation of wave formation, run-up and overtopping process utilizing the topography and bathymetry of the pre-event configuration
Whole bay	*20x20x20* *20x20x10* *15x15x10*	*6810 x 13575 x 1200*	***14,482,156; 2,251,903*** ***28,497,136; 4,129,579*** ***50,458,234; 7,254,191***	*420*	Recreation of wave propagation, inundation process and the observed trimline utilizing the topography and bathymetry of the pre-event configuration

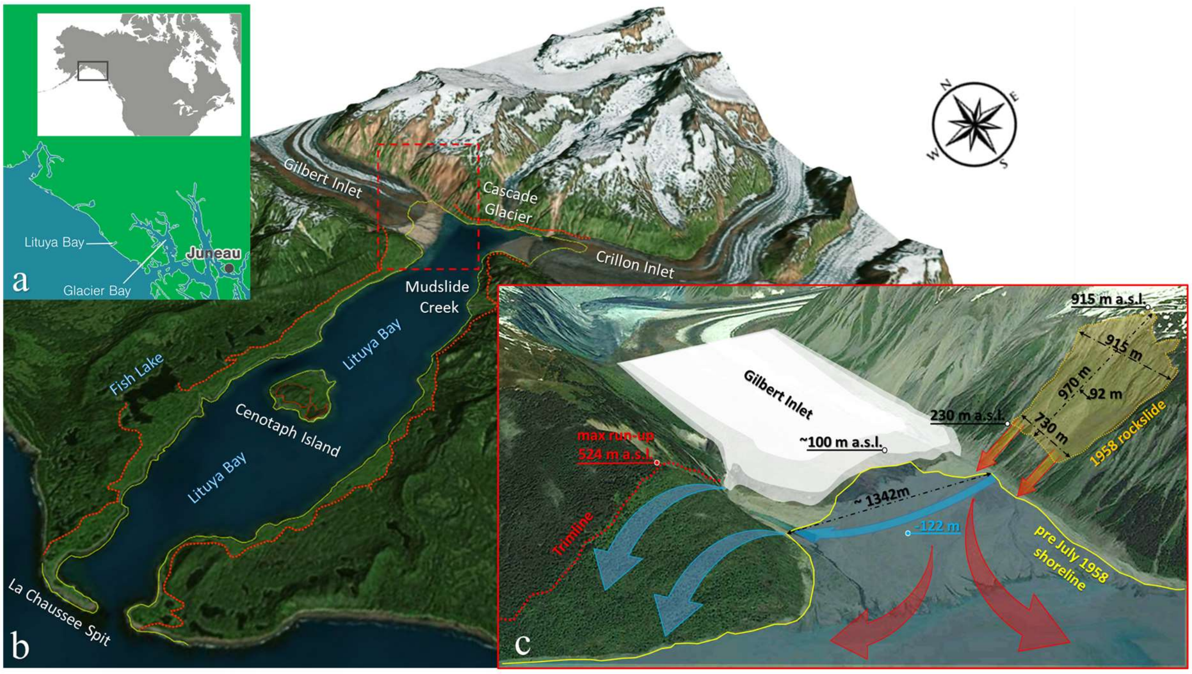

Figure 1. (a) Location of Lituya Bay, in southeast of Alaska (modified from Bridge, 2018). (b) View on Lituya Bay, the yellow line represents the shoreline before July 1958, the red line the trimline of the tsunami. (c) Gilbert Inlet showing the situation in July 1958 pre- and post-tsunami: the rockslide dimension (orange), the maximum bay floor depth of -122 m (light blue) and the maximum run-up of 524 m a.s.l. (Miller, 1960) on the opposite slope with respect to the impact area are indicated (topography data from © Google Earth Pro 7.3.2.5776, date 28/05/2015).

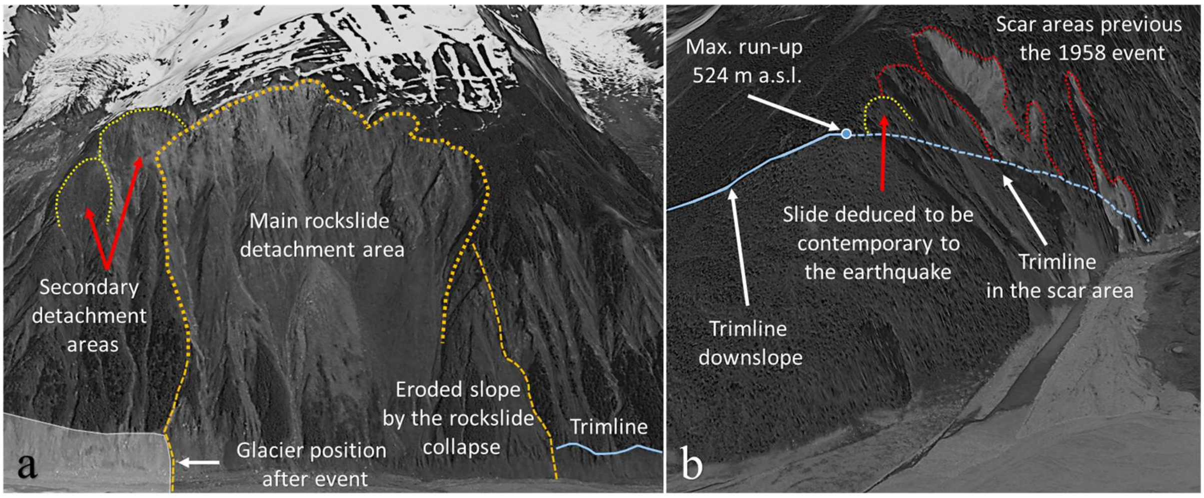

Figure 2. Rockslide source and facing opposite slope of the maximum run-up (info according from the interpretation of Ward and Day, 2010, refer to Figure 1). (a) NE-directed overview of rockslide detachment area. (b) NW-directed overview towards the Gilbert Inlet; the blue line shows the tsunami trimline on Gilbert Head as mapped by Miller (1960); red dotted lines are related to scar areas pre-1958 event on this slope; yellow dotted lines are related to a slide supposed to be coincident to the earthquake of 9 July 1958 as interpreted by Miller, 1960 (topography data from © Google Earth Pro 7.3.2.5776, date 28/05/2015).

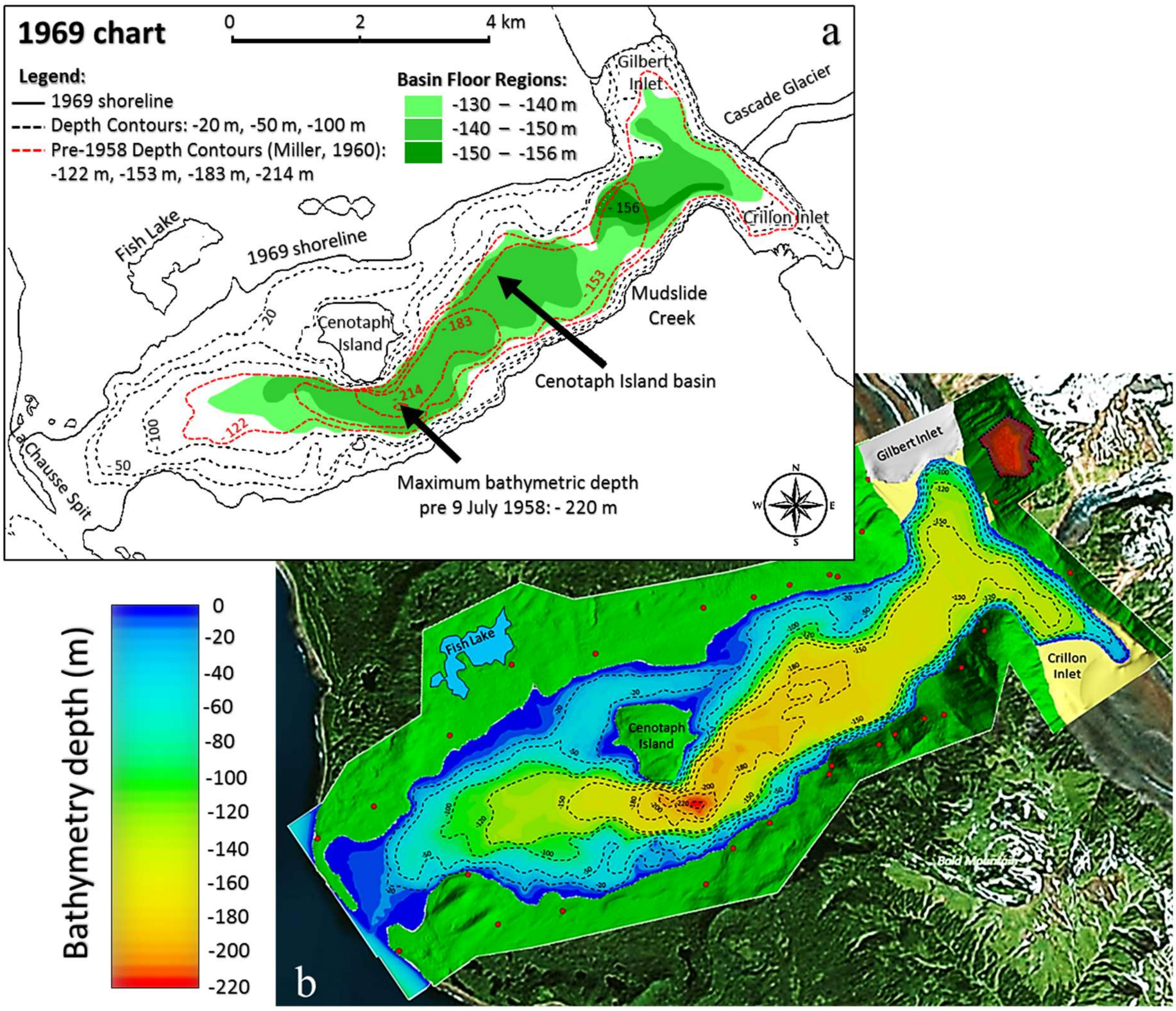

Figure 3. (a) The 1969 chart, based on a 1959 survey, highlights the flat bay floor (max. depth about -150, -156 m) relative to the pre-1958 data (red dashed lines, max depth of -220 m) provided by Miller (1960) (modified from Ward and Day, 2010, refer to Figure 8). (b) Reconstruction of the Lituya Bay pre-1958 bathymetry based on data from U.S. Coast and Geodesic Survey: Survey id: H04608, 1926 and Survey id: H08492, 1959; DTM available from DGGS Elevation Portal of Alaska (background topography from © Google Earth Pro 7.3.2.5776).

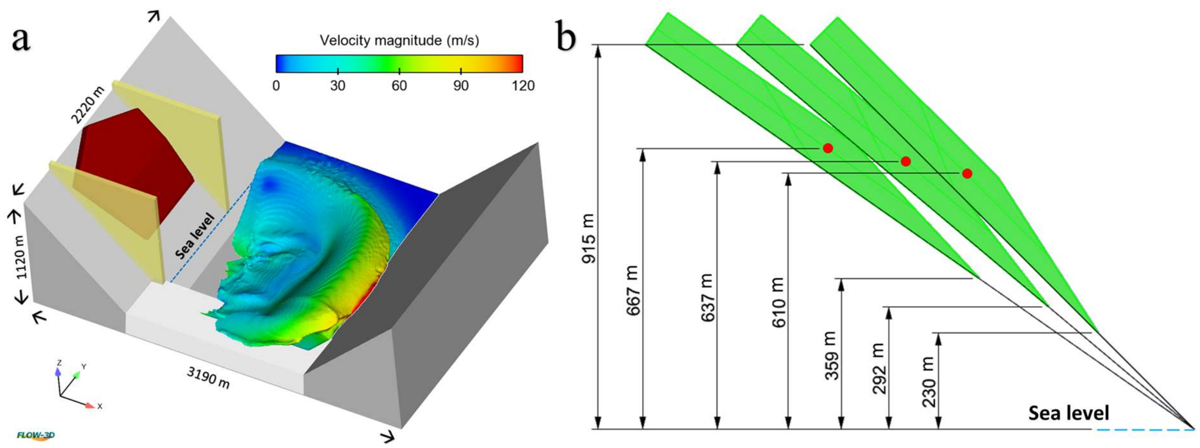

Figure 4. (a) Configuration of the bay head at Gilbert Inlet used for concept model analysis (for a slope angle of 45 degrees). The initial position of the impacting fluid (brown), the glacier (white) and the two constraining walls are shown. The wave propagation and flow velocity magnitude contours (total velocity considering all the vector components) before impacting the opposite slope are illustrated (simulation time = 32 s). (b) Illustration showing the position of the impacting fluid and its related center of gravity (red spot) for different slope angles (35°-40°-45°).

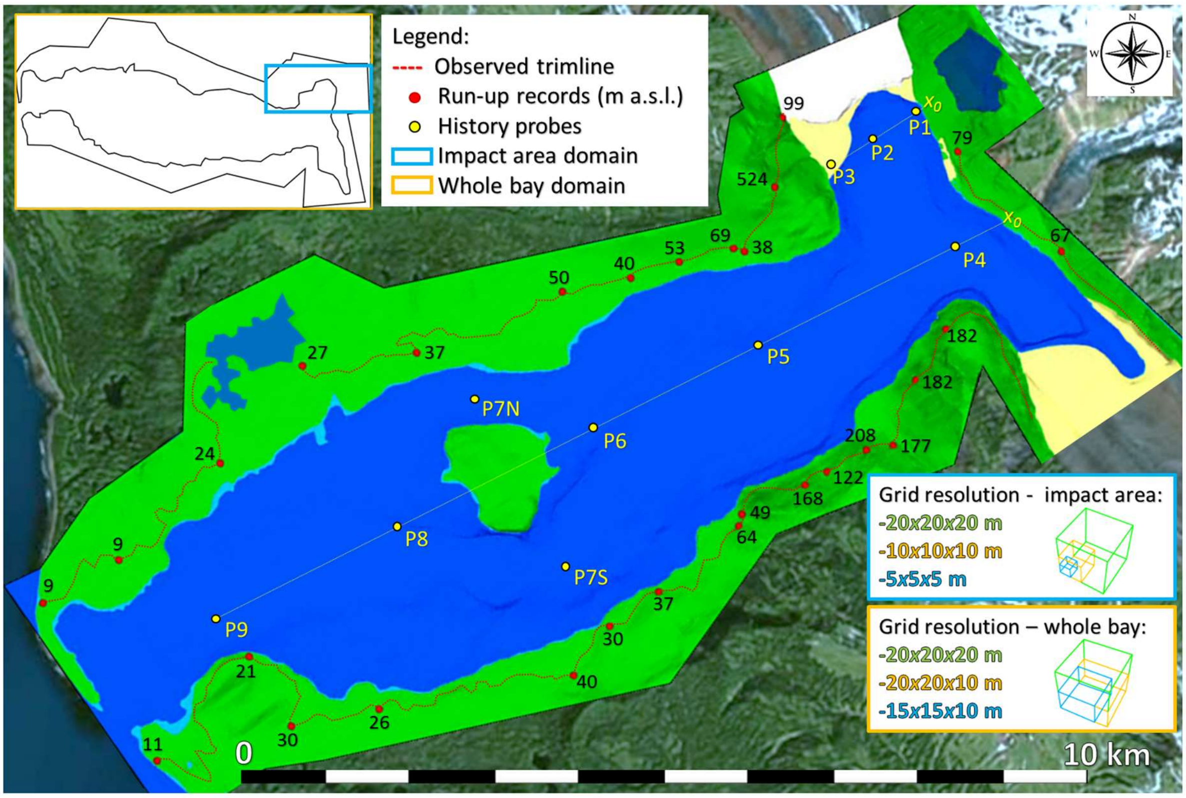

Figure 5. Model set up, covering impact area (light blue rectangle) and the whole bay (orange rectangle); the different adopted grid resolutions are shown. Observation gauges (history probes, yellow points P) represent water level gauges; the observed trimline (red dotted lines) and the documented run-up values along the bay (red spots) are used for model validation (background topography from © Google Earth Pro 7.3.2.5776).

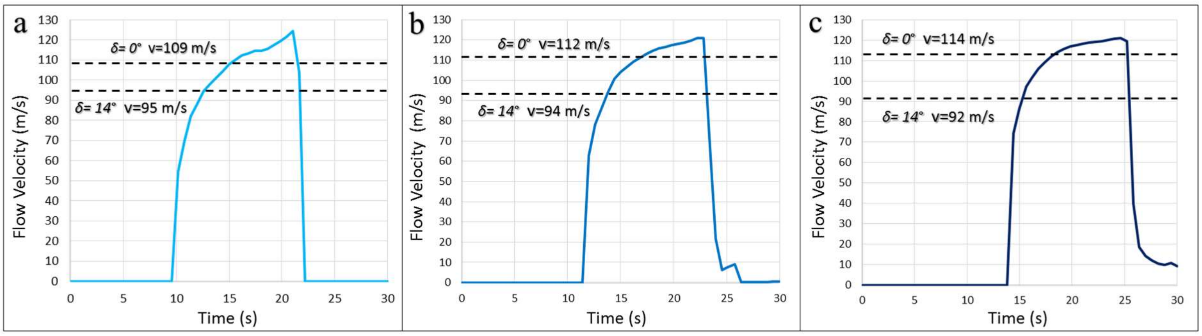

Figure 6. Impact velocity distribution versus time for the impacting fluid considering different slope angles of (a) 45°, (b) 40° and (c) 35°. The lower and upper limits represent a reasonable velocity interval for the center of gravity of the deforming fluid, when entering the water body (from the equation 3.1 provided by Heller et al., 2009, with a dynamic bed friction angle δ of 0 and 14 degrees).

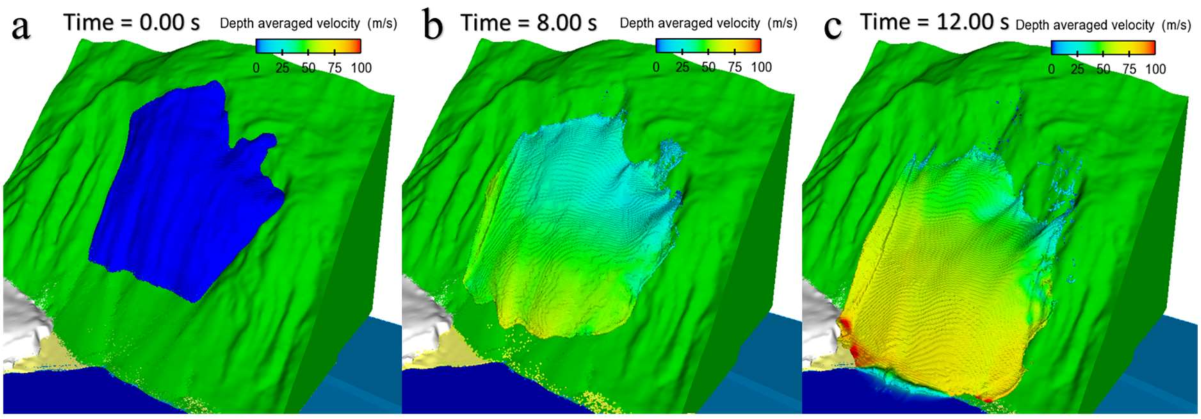

Figure 7. Fluid model at (a) 0 s, (b) 8 s and (c) 12 s impacting the sea – colored by the depth-averaged velocities in (m/s) with a range 0-100 m/s. Uniform grid resolution of 5 m.

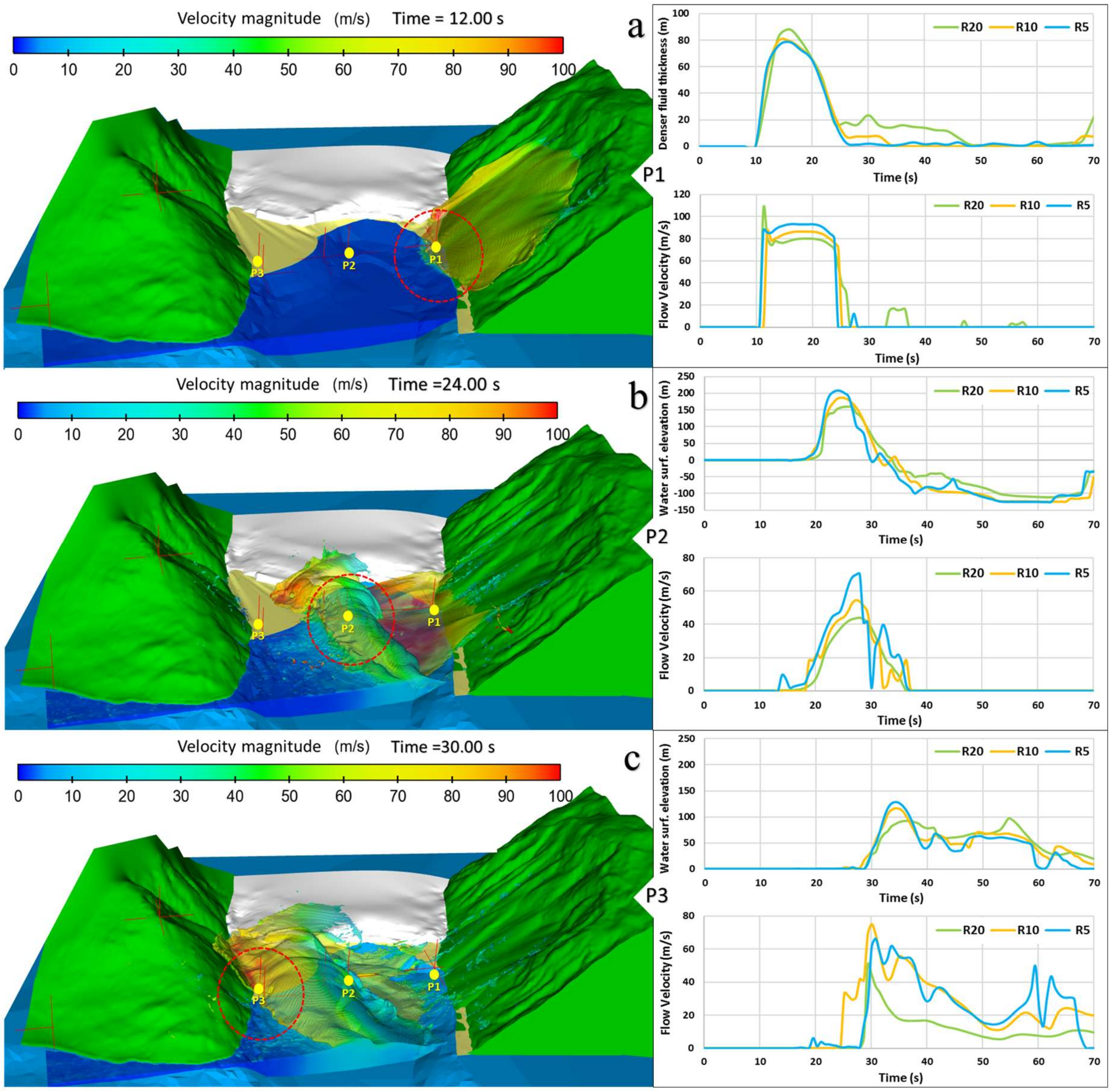

Figure 8. Wave formation and propagation in the impact area using the second order approach for the density evaluation. Observation gauges P1, P2, P3 are set to verify the water surface elevation and flow velocity magnitude. Their trends are shown in the graphs for different grid resolutions (R: 5-10-20 m). More accurate results are obtained using the grid resolution of 5 m (sky-blue line, R5).

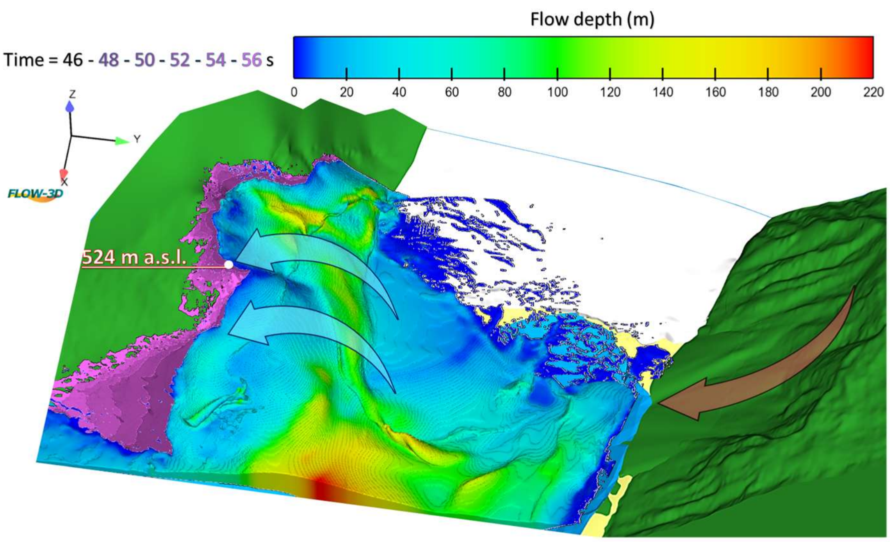

Figure 9. Impulse wave run-up on the opposite slope. At time step 46 seconds the wave reaches the maximum observed elevation of 524 m a.s.l. (flow depth contours). A part of the wave body overtops the hill and proceeds its path in a diagonal direction with respect to the slope gradient (shown by the different shades of purple for the time steps of 48-50-52-54-56 seconds).

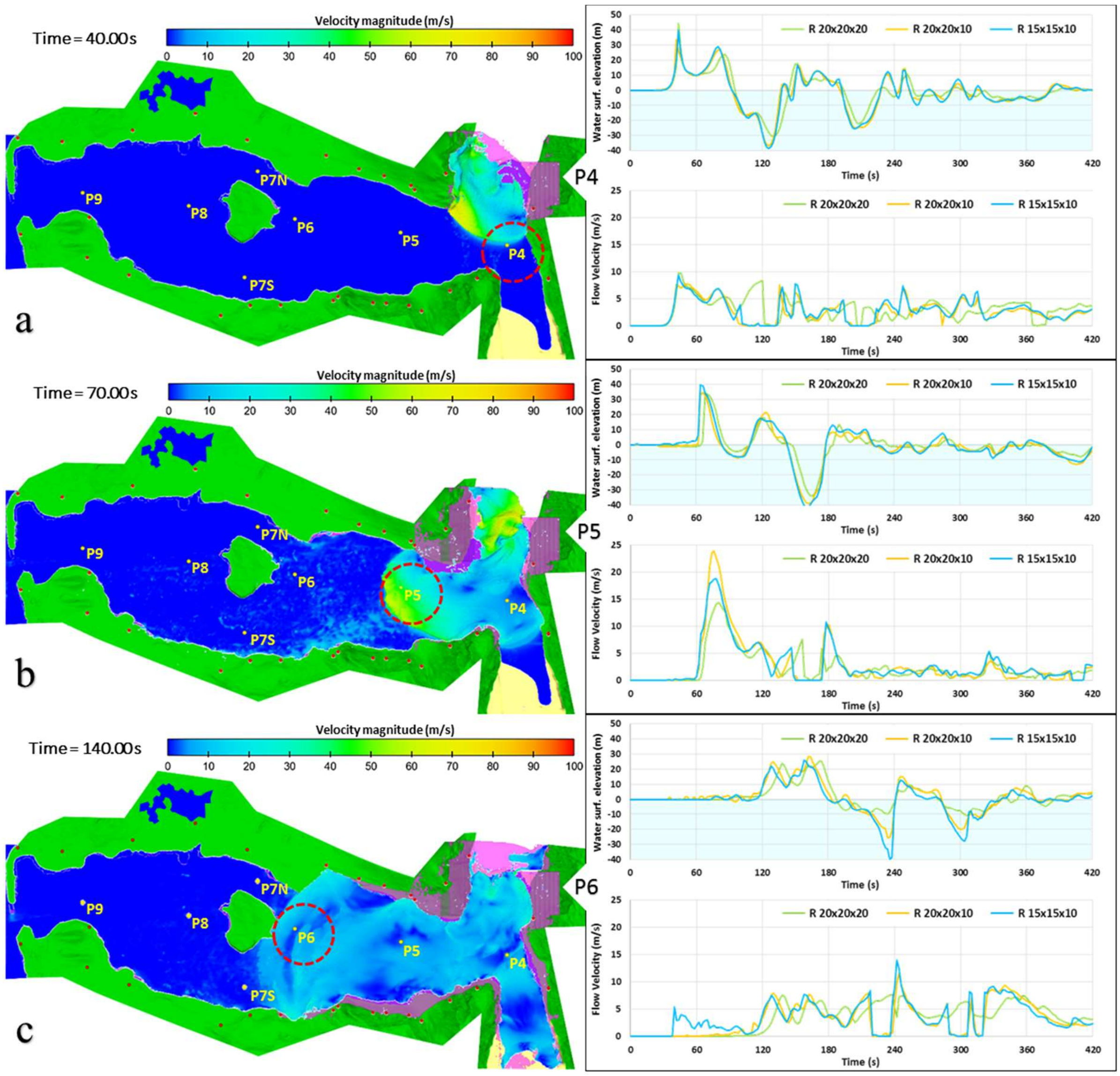

Time = 40.00s
Velocity magnitude (m/s)
P4
P5
P6
P7N
P7S
P8
P9
a
Time = 70.00s
b
Time = 140.00s
c
Water surf. elevation (m)
Flow Velocity (m/s)
Time (s)
R 20x20x20
R 20x20x10
R 15x15x10

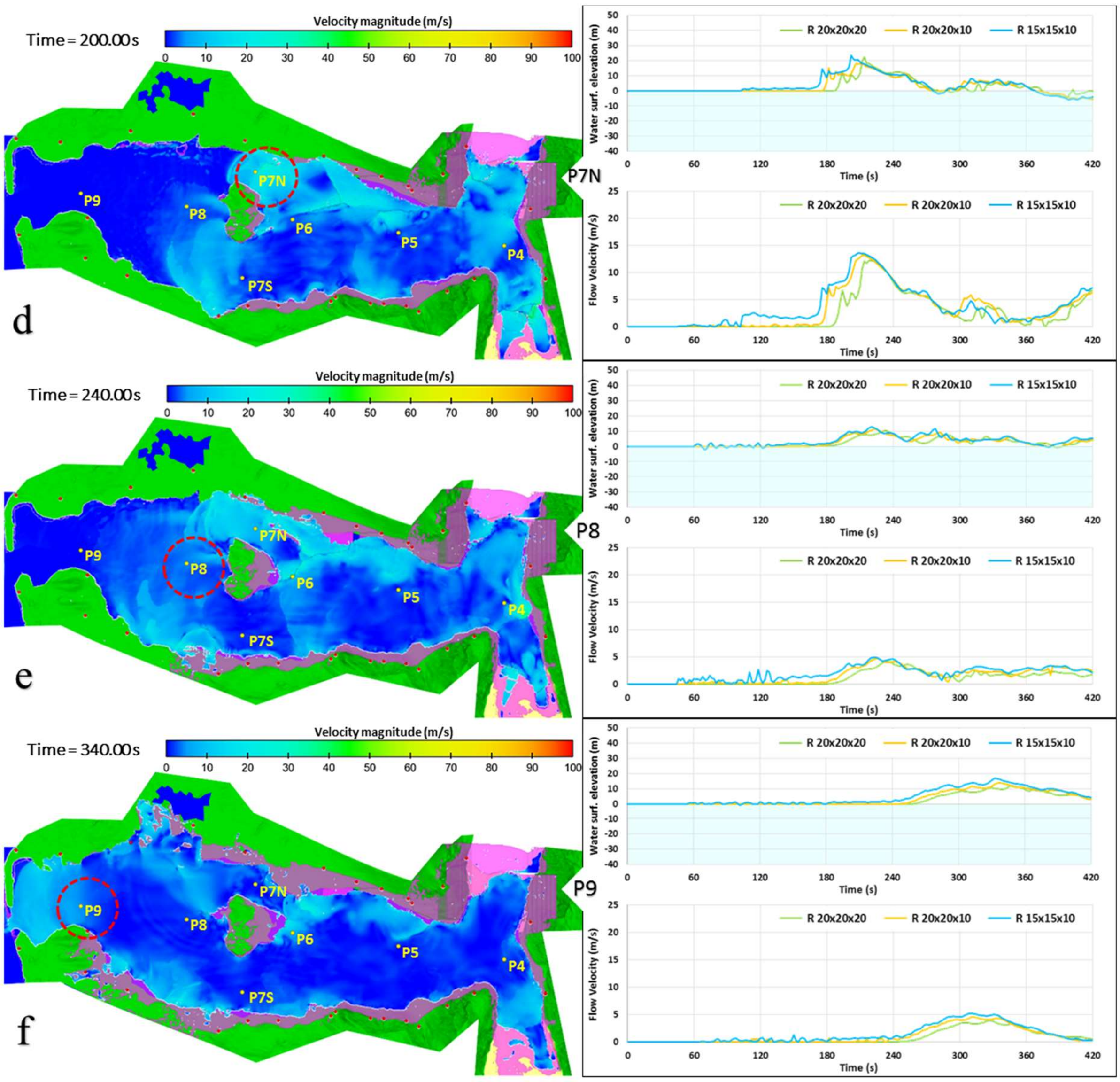

Figure 10. After the fluid impact into the sea, the wave propagates and floods the inner land along the bay. The images show the flow velocity magnitude at (a) 40 s, (b) 70 s, (c) 140 s, (d) 200 s, (e) 240 s and (f) 340 s. Different observation gauges are set to check the wave attenuation during wave propagation. The trend of the water surface elevation and flow velocity are shown in the graphs for the related observation gauge, adopting different non-uniform grid resolutions (R: 20x20x20, 20x20x10 and 15x15x10 m). The purple color on the inland represent the inundated areas while the wave propagates.

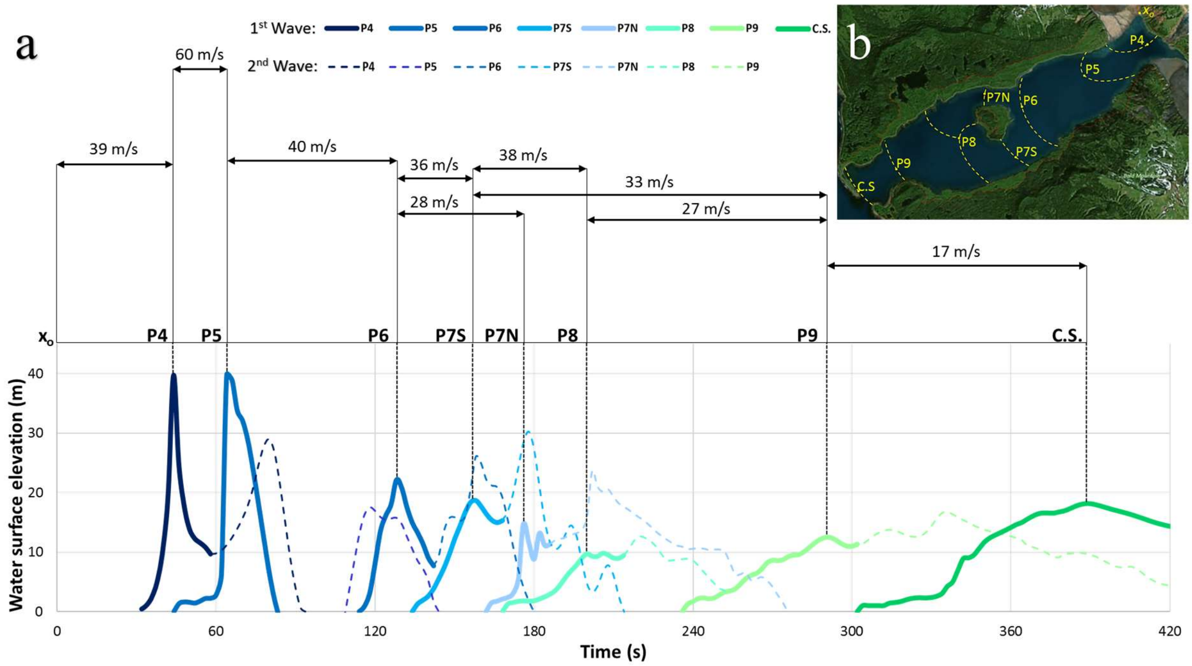

Figure 11. (a) Wave attenuation process during its propagation in the bay. The first and the second wave fronts are represented by the full and dashed lines respectively. Mean wave propagation velocity is estimated starting from the records at every gauge, considering the position of the first wave front displayed
5 **in (b) at the moment of its passage upon the gauges and path lines to estimate the distance of propagation.**

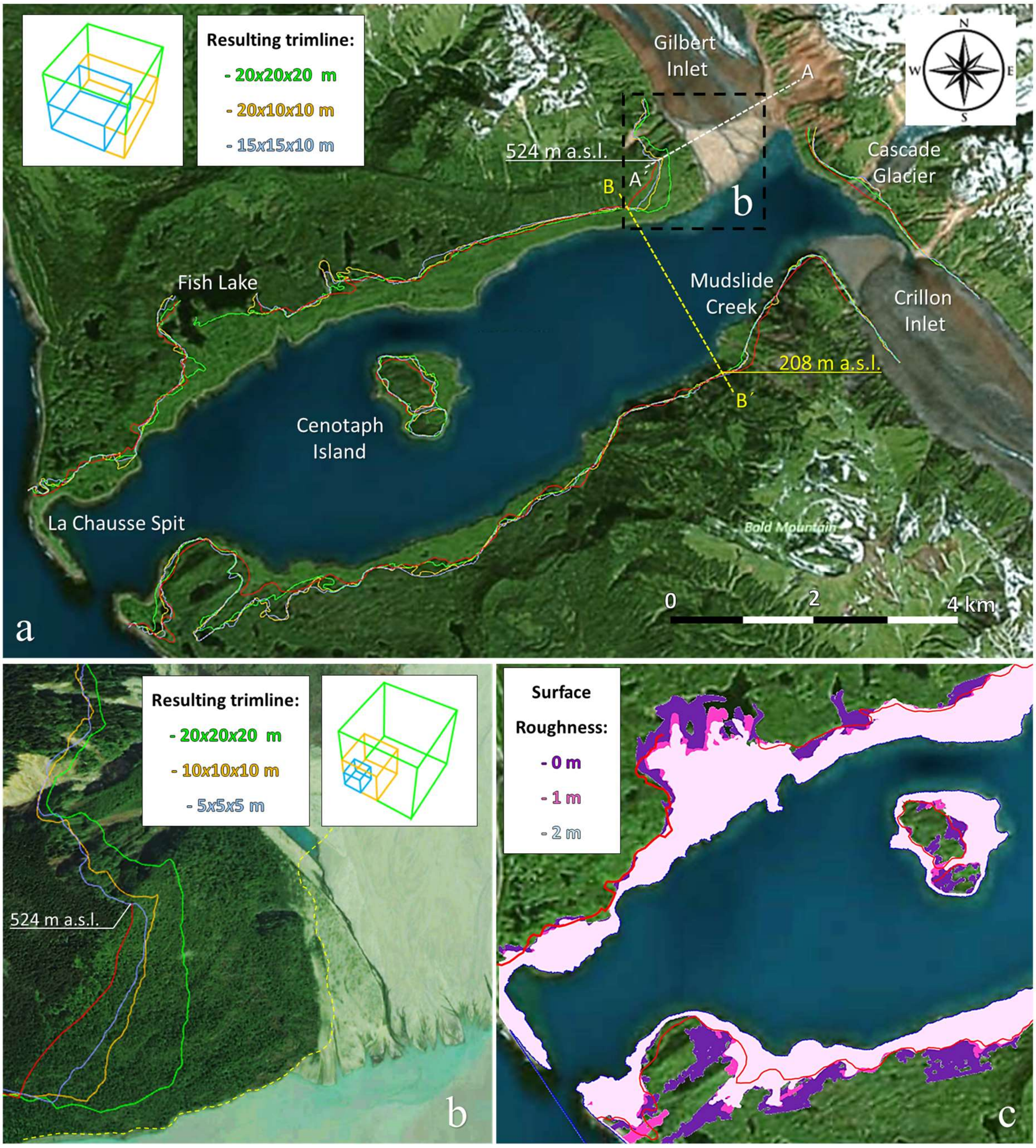

Figure 12. (a) Different results of the inundated area and the related trimline, with respect to the observed data (red line), for different grid resolutions and relative roughness equal to 0 m. Sections are reported in Figure 13 (b) At Gilbert Inlet, the resulting trimlines are defined from the grid resolutions used for the impact area simulations (20-10-5 m) and relative roughness equal to 0 m.; the yellow dashedd line represents the shoreline before the tsunami event. (c) The resulting inundation area varies in function of the selected relative roughness of 0-1-2 m for the topographic surface (background topography from © Google Earth Pro 7.3.2.5776).

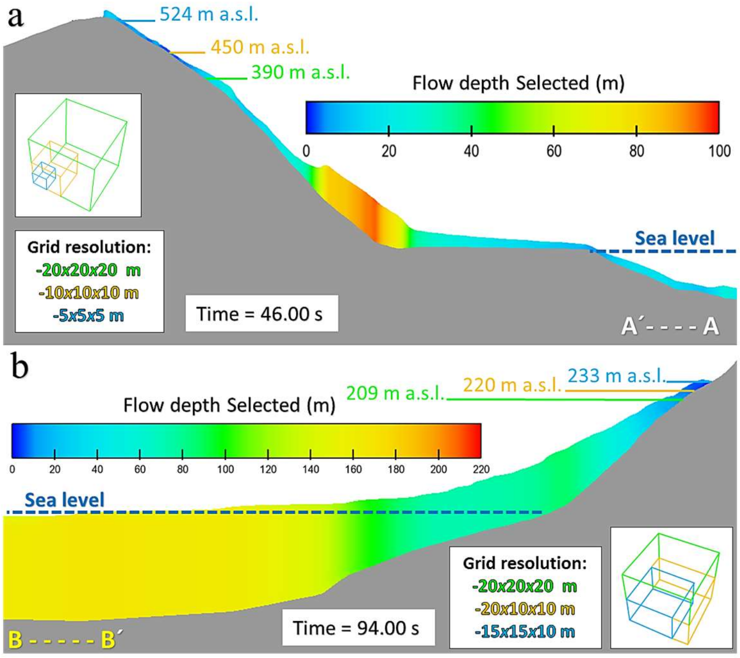

Figure 13. Maximum wave run-up resulting from different grid resolutions (referred cross section in figure 12) (a) In the impact area the maximum resulting run-up of 524 m a.s.l. relates to the 5 m uniform mesh size. (b) The maximum wave run-up results in 233 m a.s.l. for a non-uniform mesh size of 15x15x10 at the Mudslide Creek (observed run-up was 208 m a.s.l.).

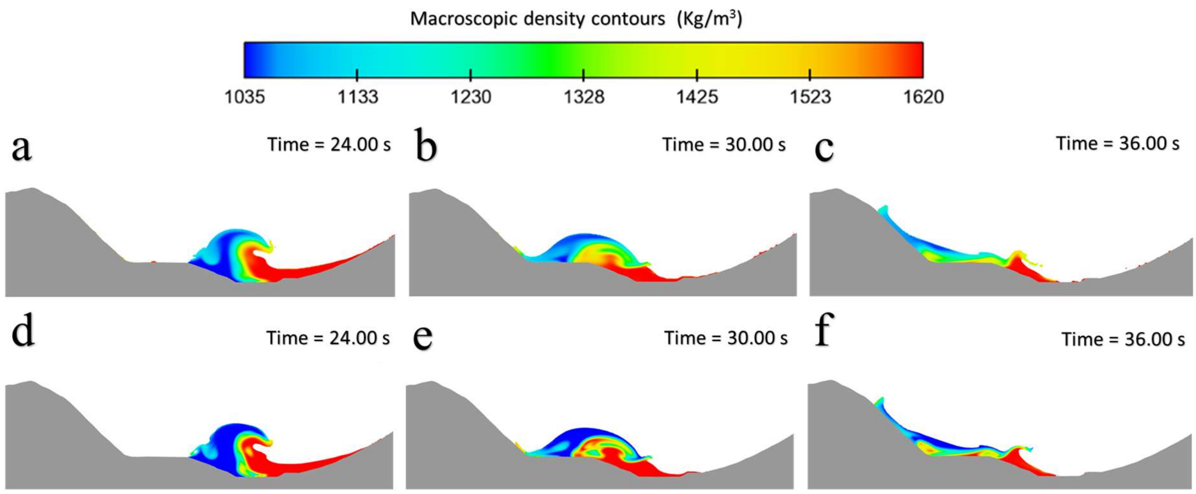

Figure 14. Vertical section, for an uniform grid resolution of 5 m, at Gilbert Inlet showing the interaction and the mixing process between the two fluids adopting the first order approach (a, b, c) and the second order approach (d, e, f) for the density evaluation.

Table 2: Summary of the simulations setup and goal descriptions.

Model	Resolution (m)	Cells number	Domain extent (m)	Sim. Time (s)	Description
Simplified analysis	*12.7x9x8*	*250,250,140*	*3187 x 2225 x 1122*	*60*	Test the rockslide concept and its effect on the wave formation and run-up in the simplified bucket model
Impact area	*20x20x20* *10x10x10* *5x5x5*	*80,200,60* *160,400,120* *320,800,240*	*1600 x 4000 x 1200*	*70*	Recreate the wave formation, run-up and overtopping process utilizing the topography and bathymetry pre-event configuration
Whole bay	*20x20x20* *20x20x10* *15x15x10*	*260,220,60* *260,220,120* *454,905,120*	*6810 x 13575 x 1200*	*420*	Recreate the wave propagation, inundation process and the observed trimline utilizing the topography and bathymetry pre-event configuration

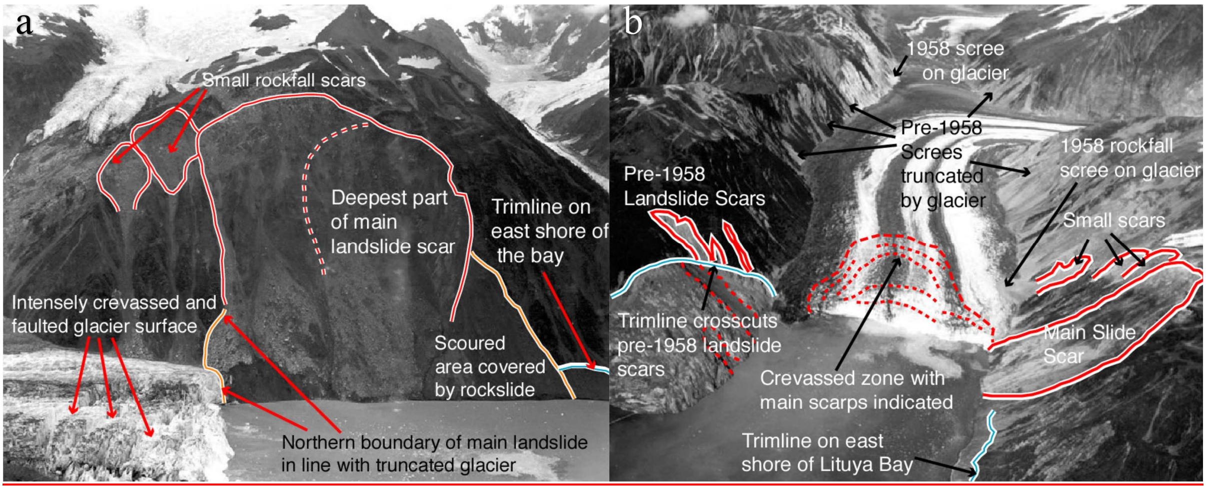

Figure 2. Pictures of Miller's rockslide scar and Lituya glacier (1960), Ward and Day interpretation (2010). (a) NE overview of rockslide scar and the Gilbert Glacier. (b) NW overview up the Gilbert Glacier; red dashed lines represent new scarps on the glacier; the blue line shows the tsunami trimline on Gilbert Head as Miller (1960) mapped.

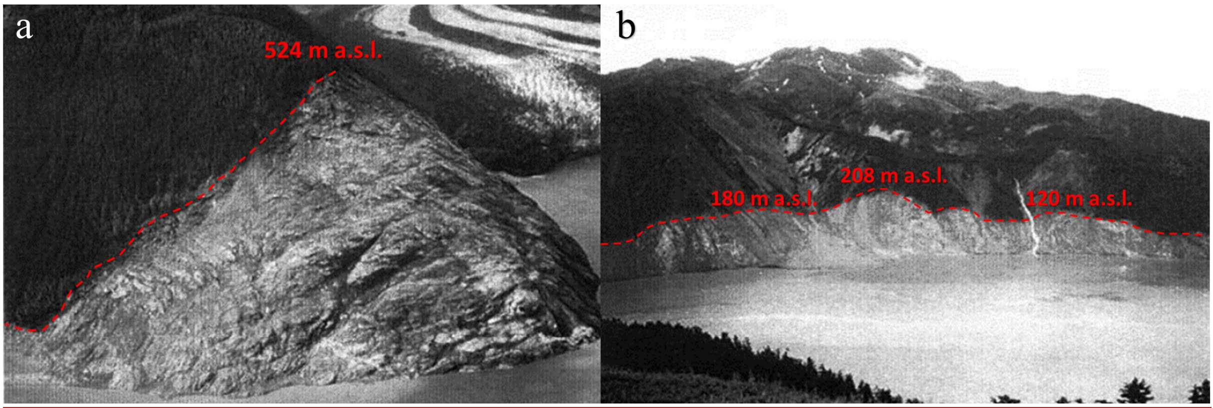

Figure 3. Highest marks on giant wave trimlines in 1958. (a) North overview of the maximum run-up at the altitude of 524 m a.s.l. (b) South overview of the second highest run-up and trimline in the Mudslide Creek location resulting in a maximum altitude of 208 m a.s.l. (photos: courtesy of USGS, modified from Fritz et al., 2001).

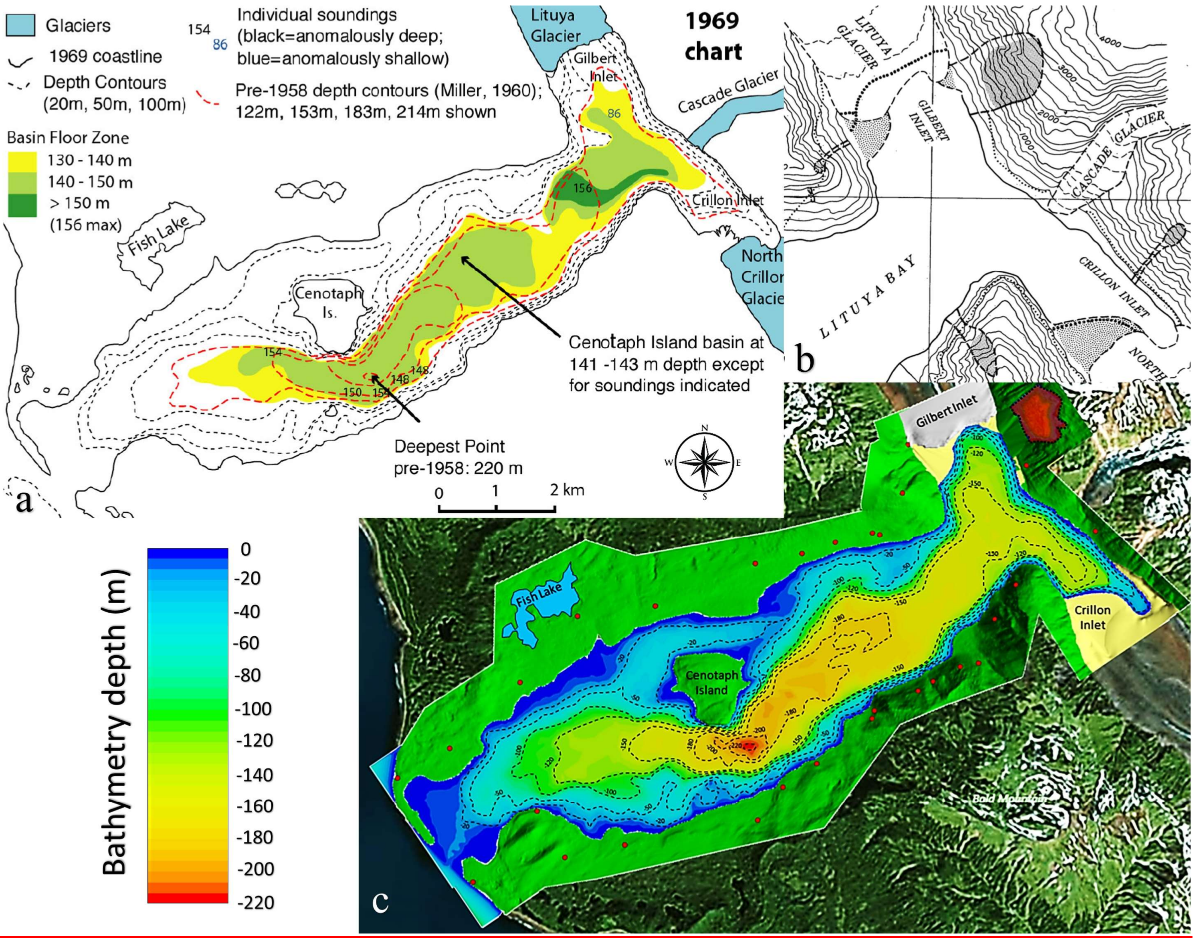

Figure 4. (a) The 1969 chart, based on a 1959 survey, highlights the flat bay floor (max. depth about 150-156 m), respect the pre-1958 data (red dashed lines, max depth of 220 m) provided by Miller (1960) (modified from Ward and Day, 2010). (b) Map of Lituya Bay's head, displaying slides, coastline and glacier front shifts, and the trimline of the tsunami in 1958 (Miller, 1960). (c) Reconstruction of the Lituya Bay pre1958 bathymetry based on data from U.S. Coast and Geodesic Survey: Survey id: H04608, 1926 and Survey id: H08492, 1959; DTM available from DGGS Elevation Portal of Alaska (background topography from © Google Earth Pro 7.3.2.5776).

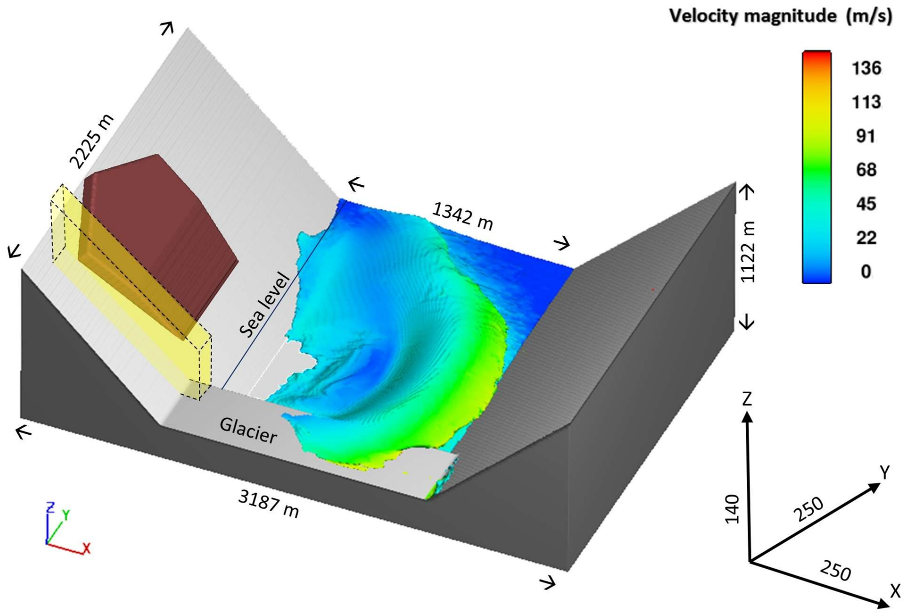

Figure 5. Configuration of the bay head at Gilbert Inlet used for simplified simulations. The initial position of the rockslide (brown), the glacier (grey) and one constraining wall on the right side of the rockslide (yellow) are showed. The wave propagation and its velocity magnitude (total velocity considering all the vector components) before impacting the opposite slope are illustrated (simulation time = 32 s).

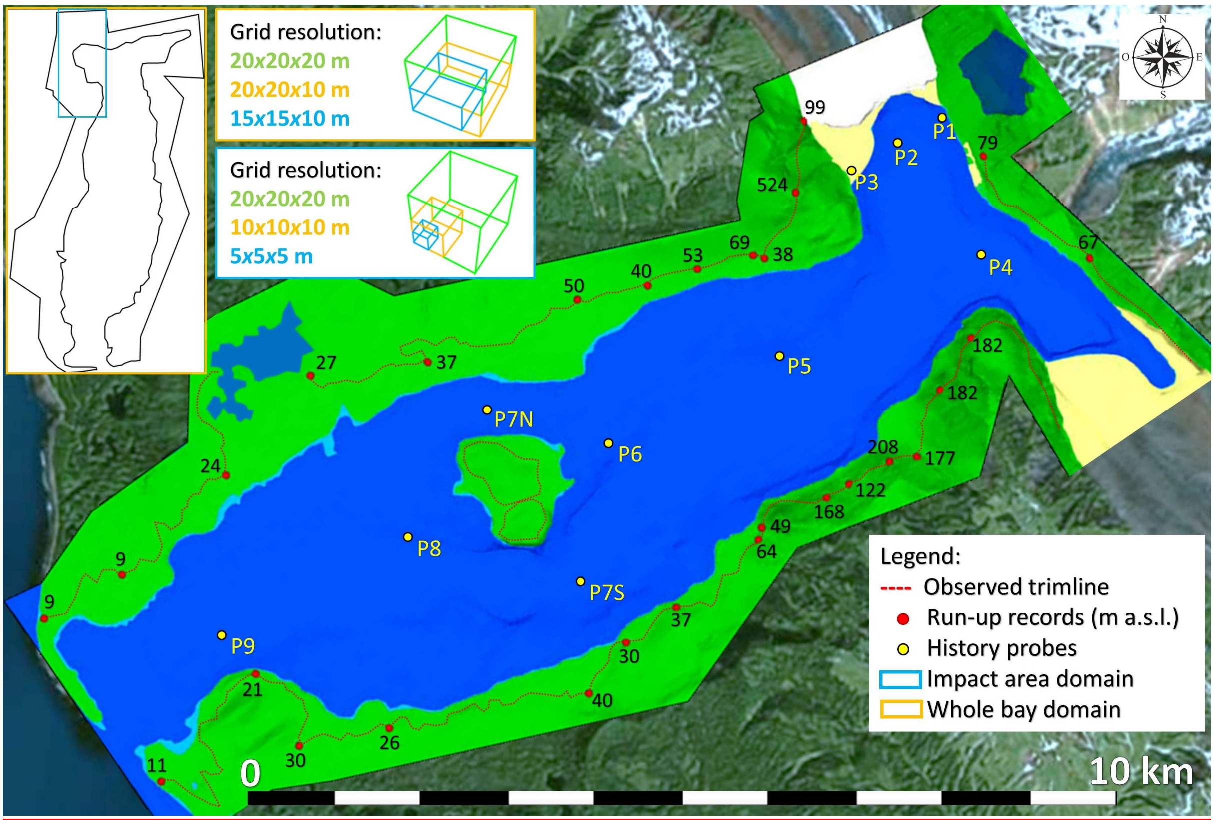

Figure 6. Model set up, covering impact area (light blue rectangle) and the whole bay (orange rectangle); the different adopted grid resolutions are showed. Observation gauges (history probes, yellow points P) represent water level gauges; the observed trimline (red dashed lines) and the documented run-up values along the bay (red spots) are used for model validation (background topography from © Google Earth Pro 7.3.2.5776).

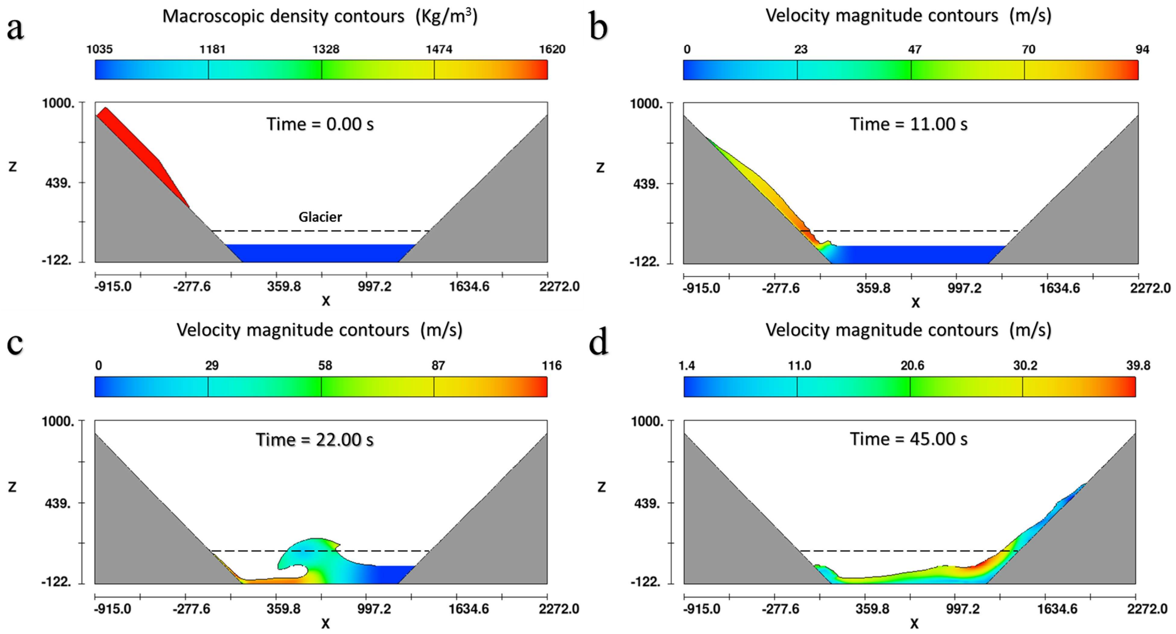

<u>**Figure 7.** Simplified simulations results presented as a vertical section along the main wave propagation direction. (a) Position of the rockslide before the failure (red). (b) Moment of the initial impact in the water body, the rockslide reaches an impact velocity of 94 m/s. (c) Formation and propagation of the wave. (d) Run-up at the opposite slope.</u>

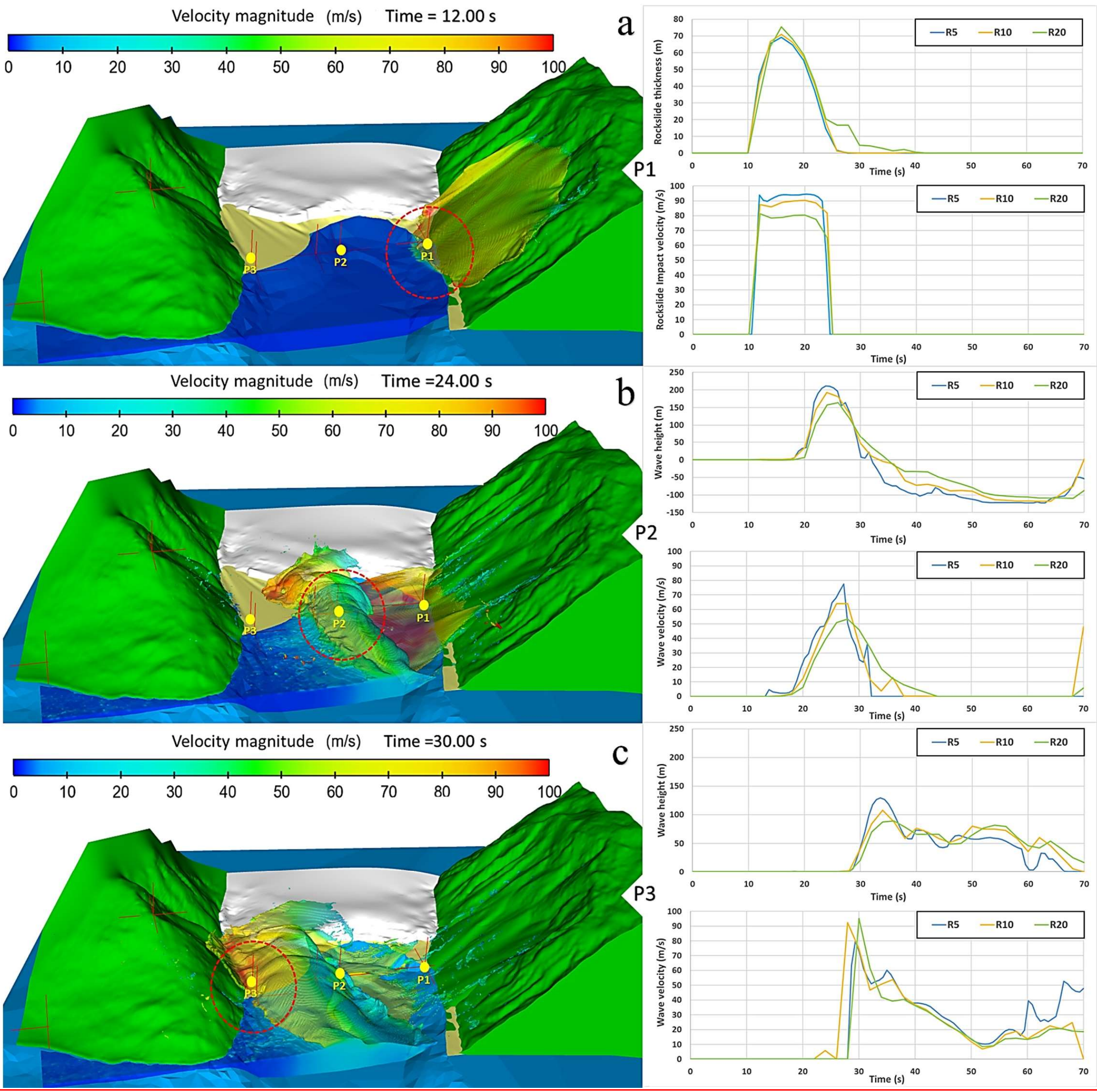

Figure 9. Wave formation and propagation in the impact area using the second order approach for the density evaluation. Observation gauges P1, P2, P3 are set to check the wave features as height a.s.l. and wave velocity magnitude. The wave features trends are showed in the graphs for different grid resolutions (R: 5-10-20 m). More accurate results are obtained using the grid resolution of 5 m (sky-blue line, R5).

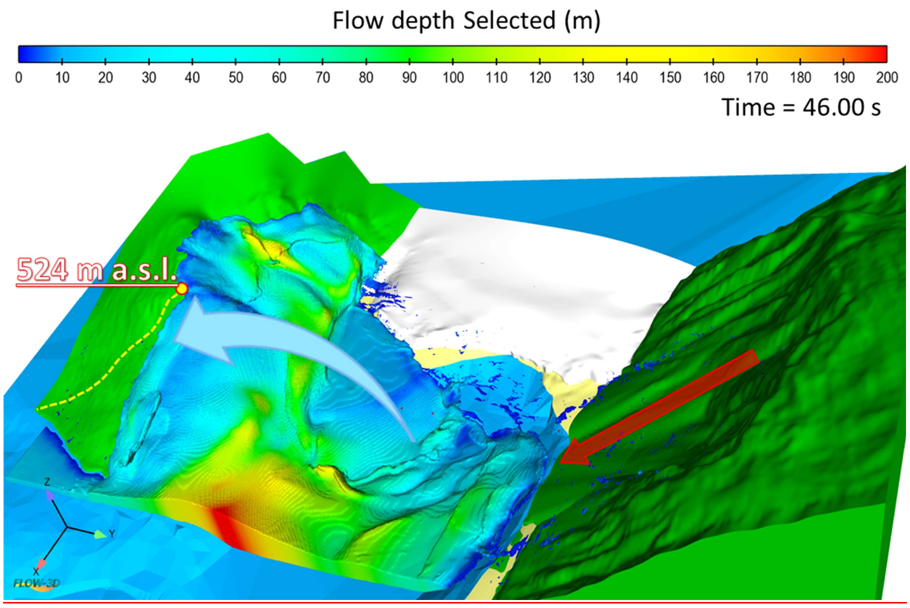

Figure 10. Resulting impulse wave run-up on the opposite slope (reaching the maximum elevation observed 524 m a.s.l.). The wave overtops the hill crest and proceeds its path in a diagonal direction (yellow line) with respect the slope dip.

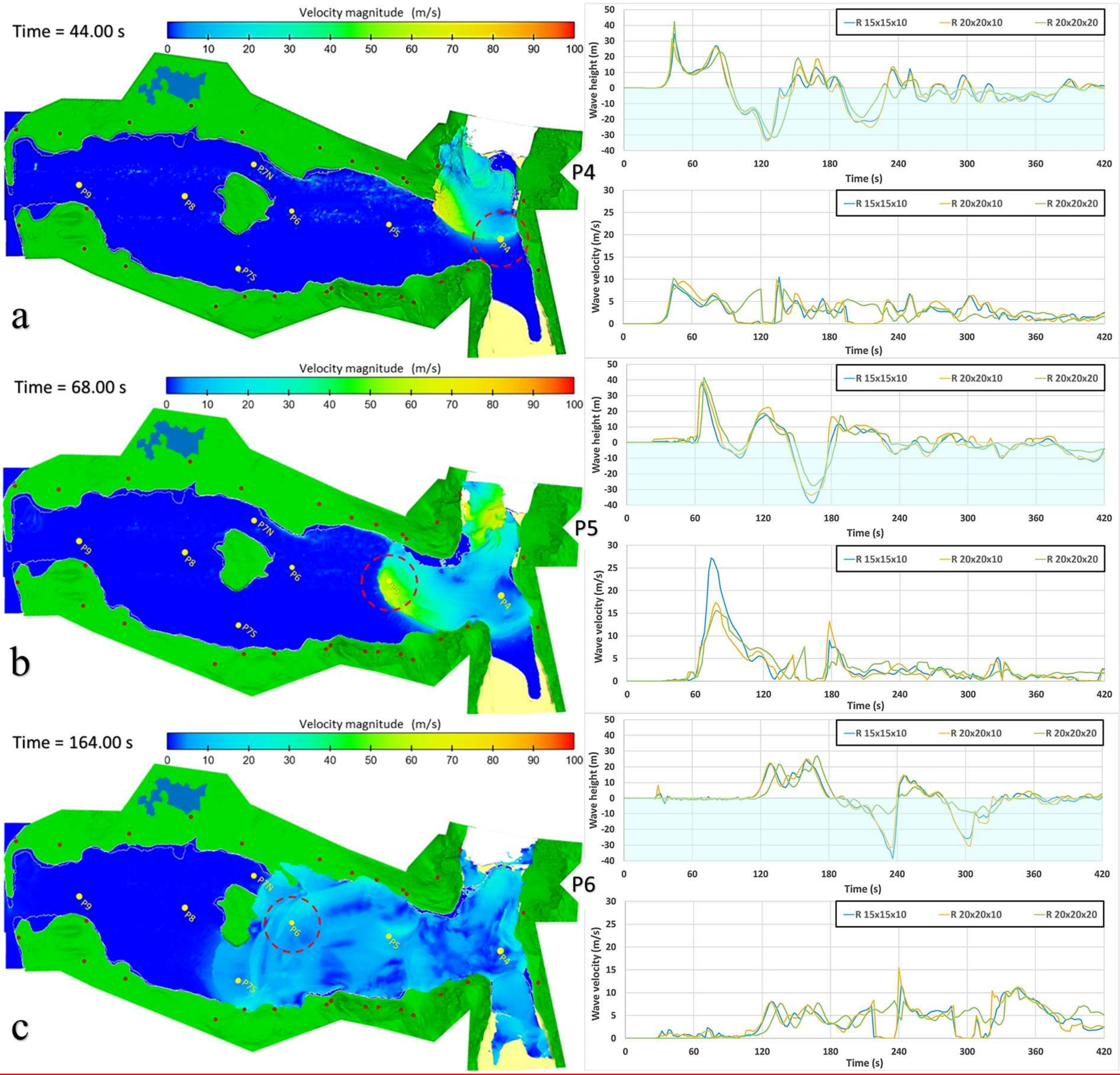

Time = 44.00 s
Velocity magnitude (m/s)
P4
a
Time = 68.00 s
P5
b
Time = 164.00 s
P6
c
Wave height (m)
Wave velocity (m/s)
Time (s)
R 15x15x10
R 20x20x10
R 20x20x20

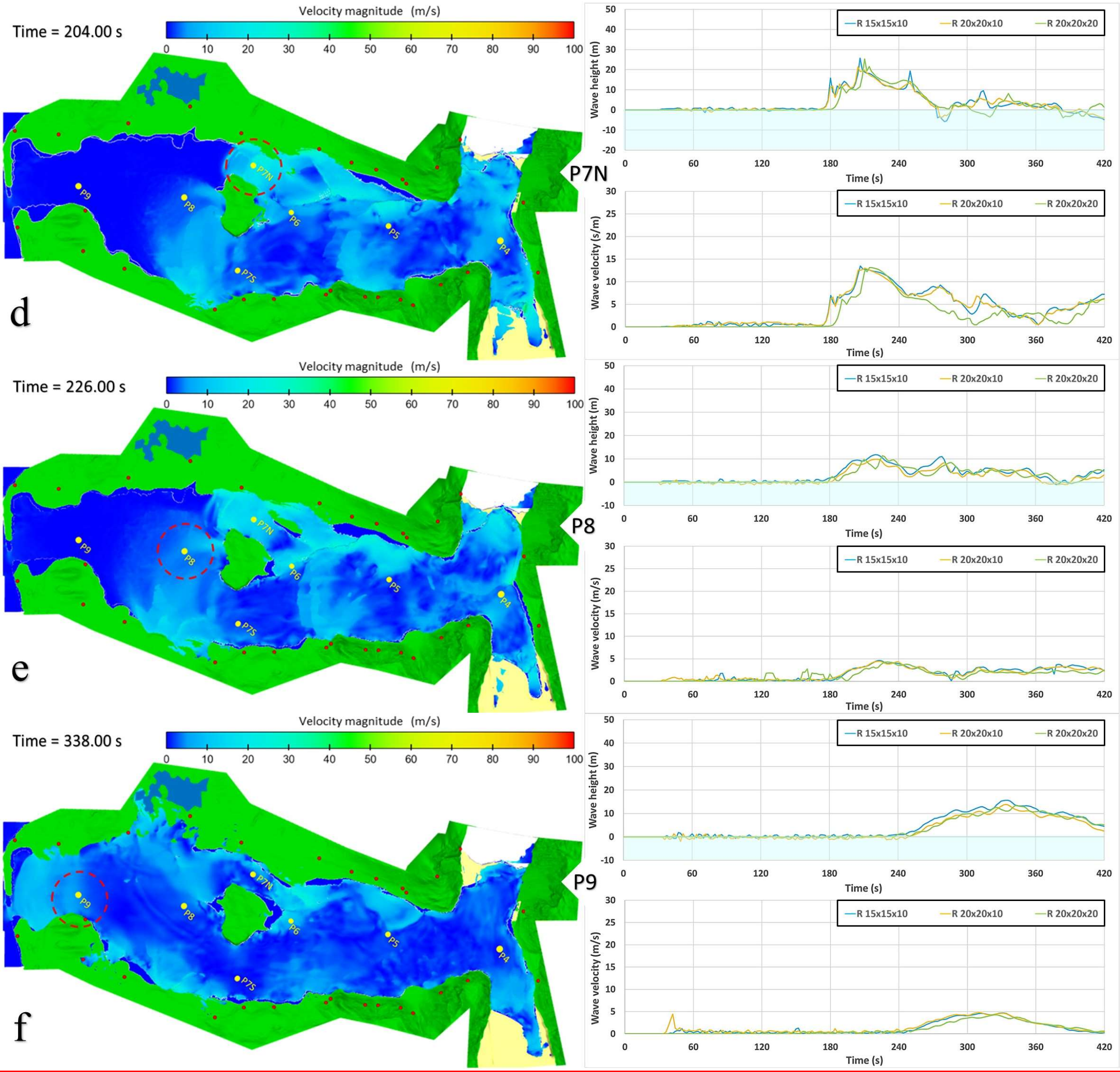

Figure 11. After the rockslide´s impact into the sea, the wave propagates and floods the inner land along the bay. The images show the wave velocity magnitude at (a) 44 s, (b) 68 s, (c) 164 s, (d) 204 s, (e) 226 s and (f) 338 s. Different observation gauges are set to check the wave attenuation during wave propagation. The trend of the wave height a.s.l. and its velocity are showed in the graphs for the related observation gauge, adopting different non-uniform grid resolutions (R: 20x20x20, 20x20x10 and 15x15x10 m).

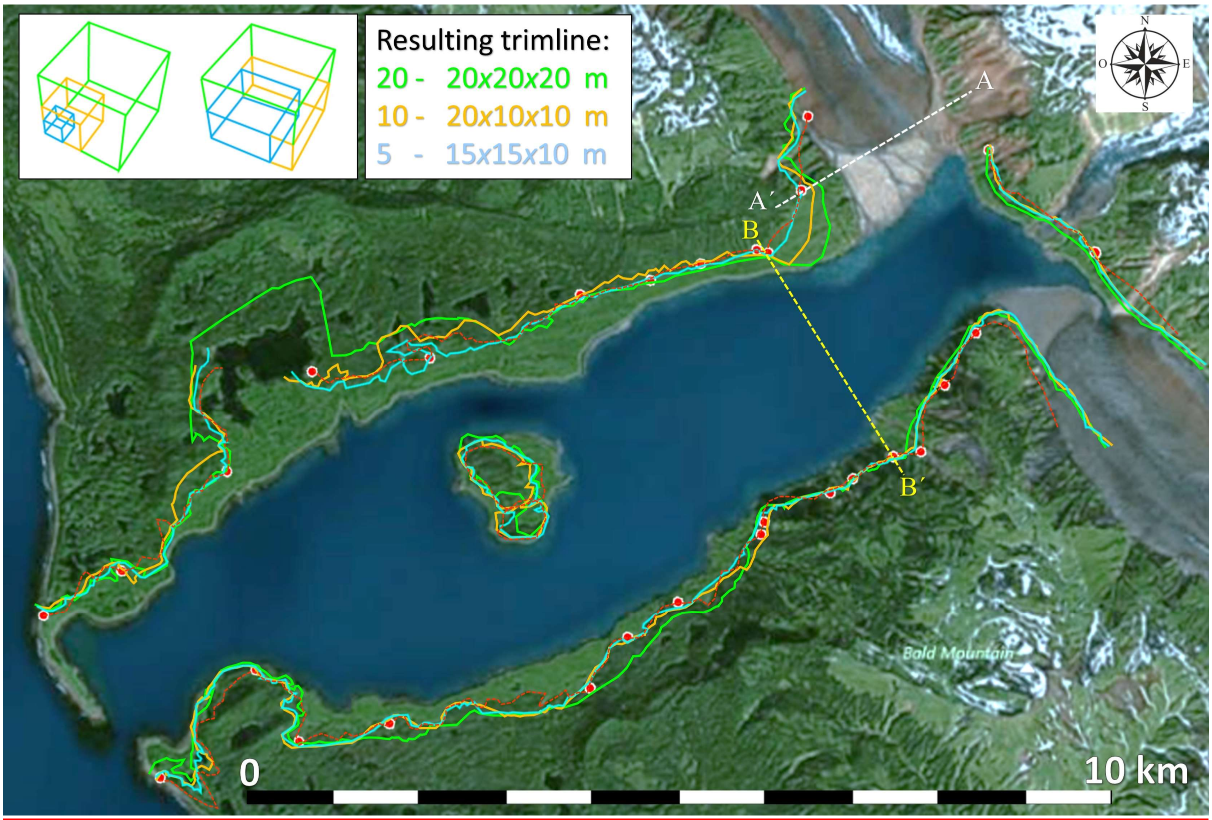

Figure 12. Different results of the flooded area and the related trimline for different grid resolutions. At Gilbert Inlet, the resulting trimlines are defined from the grid resolutions used for the impact area simulations (20-10-5 m). The resulting trimline, along the all bay, using a mesh size of 15x15x10 m, is the one closest to the actual observed trimline (background topography from © Google Earth Pro 7.3.2.5776). Sections are represented in figure 14.

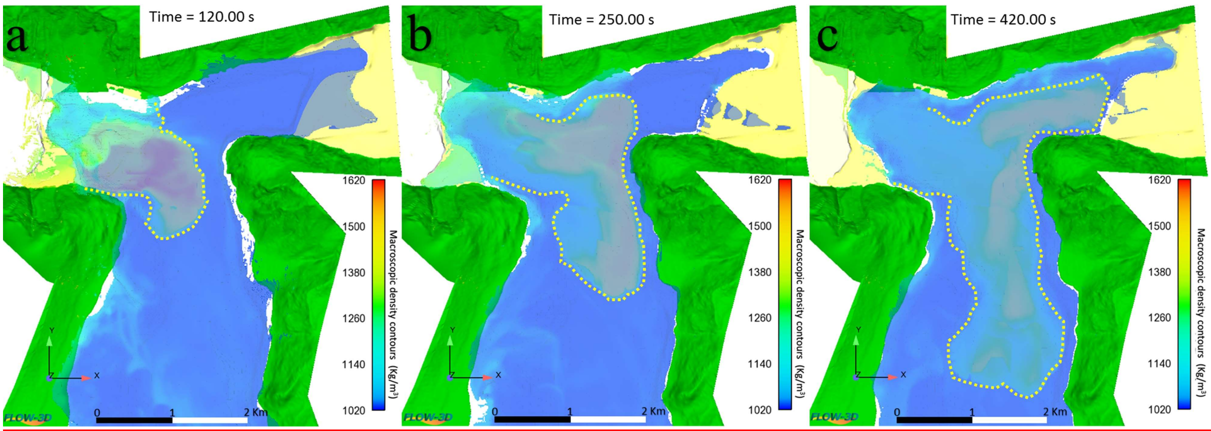

Figure 13. Rockslide material propagating along the bay floor. After 420 s the material still expands with a velocity of 8 ms^{-1}, reaching a distance of almost 5 km from the impact point (c). The bulk slide density decreases during the propagation from 1620 kgm^{-3} to 1260 kgm^{-3}.

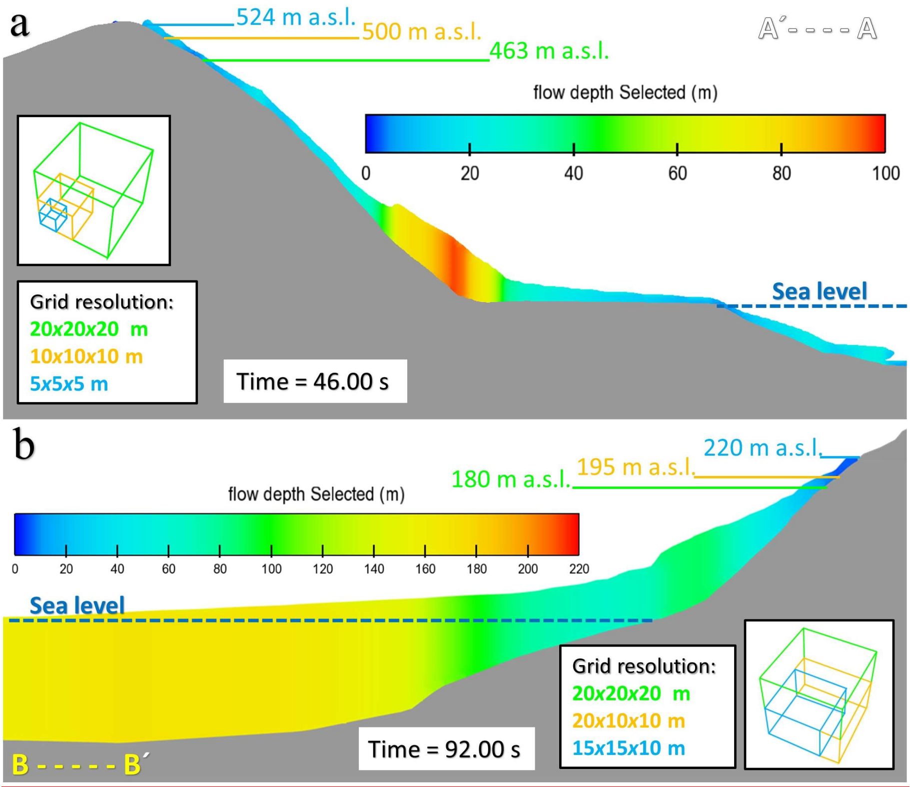

Figure 14. Maximum wave run-up resulted from different grid resolutions. (a) In the impact area the maximum resulting run-up of 524 m a.s.l. for 5 m uniform mesh size. (b) At the Mudslide Creek the second highest observed run-up (208 m a.s.l.) is overreached resulting in 220 m a.s.l. for a non-uniform mesh size of 15x15x10.

5